İSTANBUL TECHNICAL UNIVERSITY ★ INSTITUTE OF SCIENCE AND TECHNOLOGY

DETERMINATION OF RESERVOIR ROCK WETTABILITY BY THIN LAYER WICKING APPROACH

MSc. Thesis by
Fatma Bahar ÖZTORUN, B.S.

Department: PETROLEUM AND NATURAL GAS ENGINEERING

Programme: PETROLEUM AND NATURAL GAS ENGINEERING

JUNE 2006

İSTANBUL TECHNICAL UNIVERSITY ★ INSTITUTE OF SCIENCE AND TECHNOLOGY

DETERMINATION OF RESERVOIR ROCK WETTABILITY BY THIN LAYER WICKING APPROACH

MSc. Thesis by
Fatma Bahar ÖZTORUN, B.S.

Department: PETROLEUM AND NATURAL GAS ENGINEERING

Programme: PETROLEUM AND NATURAL GAS ENGINEERING

Supervisor : Assistant Prof. Dr. H. Özgür YILDIZ

Co-advisor : Assoc. Prof. Dr. Ayhan Ali SİRKECİ

Member of jury : Prof. Dr. Mustafa ONUR

Member of jury : Assistant Prof. Dr. Şenol YAMANLAR

Member of jury : Prof. Dr. Mehmet Sabri ÇELİK

JUNE 2006

ACKNOWLEDGEMENTS

I would like to express my deep thanks to my supervisor Assistant Prof. Dr. H. Özgür Yıldız, for his advice, encouragement, kindness, patience, and thoughtfulness throughout the research and also in my academic life. I am profoundly indebted to my co-advisor Assoc. Prof. Dr. Ayhan A. Sirkeci for his steady support and motivation in writing this thesis.

I am also thankful to my committee member Prof. Dr. Mehmet Sabri Çelik for his valuable advices and his warm support in this work. Special thanks are also due to my other committee members, Prof. Dr. Mustafa Onur and Assistant Prof. Dr. Şenol Yamanlar for their advice, suggestions, and valuable comments.

Thanks to my office-mate Melih Gökmen and Rüstem Tajibaev who contributed greatly in accomplishing the experimental part of this project. Especially, I would like to express my gratitude to Mustafa Çınar, for his support during the experiments, and to Fatih Can for his motivating discussion on the subject.

I would like to thank all the faculty members and my colleagues in the Department of Petroleum and Natural Gas Engineering at Istanbul Technical University for their assistances in every possible way.

My heartfelt thanks to my family who have been of constant support, courage, and love all through my life. Finally, this thesis is dedicated to my parents and my beloved fiancé Can K. Hoşgör.

June 2006 Fatma Bahar Öztorun

TABLE OF CONTENTS

LIST OF TABLES

Page Number

LIST OF FIGURES

Page Number

LIST OF SYMBOLS AND ABBREVIATIONS

A : Cross sectional area, cm^2
d_{50} : Average particle size, μm
dt : Change in time, s
dV : Change in volume, cm^3
f : Proportions of the surface occupied by materials, unitless
F : Force, dyne
F : Helmholtz free energy of the system, Joule
F_s : Surface free energy of the system, dyne/ cm
g : Gravitational acceleration, cm/s^2
G : Gibbs free energy per unit area, Joule
l : Height of the wetting front, cm
l_T : Total length of the capillary, cm
l_1, l_2 : Respective length of the liquid columns, cm
L : Length, cm
ΔP : Pressure difference across the liquid-vapor interface in a capillary, $dyne/cm^2$
ΔP_c : Capillary pressure, $dyne/cm^2$
ΔP_e : External pressure, $dyne/cm^2$
ΔP_h : Hydrostatic pressure, $dyne/cm^2$
r : Radius of a capillary, cm
r* : Effective radius, cm
s : Surface of solid, cm^2
S : Spreading coefficient, dyne/cm
t : Time, s
T : Temperature, Kelvin
v : Laminar stationary flow, cm/s
W : Work, Joule
Z_e : Depression of the liquid in the capillary, cm
δz : Small linear displacement, cm
Γ_i : Adsorption of the element *i* in moles per unit area, $moles/cm^2$
μ_i : Chemical potential of the element, Joule
Π_e : Spreading pressure, dyne/cm
γ_S^{LW} : Lifshitz van der Waals components of the surface tension, dyne/cm
γ_S^{AB} : Acid-Base components of the surface tension, dyne/cm
γ_S^+ : Surface tension of electron acceptor components, dyne/cm
γ_S^- : Surface tension of electron donor component, dyne/cm
γ : Surface tension, dyne/cm

γ_L : Surface tension of the liquid, dyne/cm

$\gamma_{L_2L_1}$: Interfacial tension between two immiscible liquids L_1 and L_2, dyne/cm

γ_{LV} : Liquid-vapor surface tension, dyne/cm

γ_S : Surface tension of the solid, dyne/cm

γ_{SL} : Solid-liquid surface tension, dyne/cm

γ_{SL_1} : Surface tension between the liquid L_1 and a solid, dyne/cm

γ_{SL_2} : Surface tension between the liquid L_2 and a solid, dyne/cm

γ_{SV} : Solid-vapor surface tension, dyne/cm

μ : Viscosity, cp

μ_1, μ_2 : Viscosities of two immiscible liquids, cp

ρ : Density of the liquid, g/cm^3

θ : Contact angle, ^{o}

θ_{12} : The contact angle on a liquid-liquid-solid interface, ^{o}

REZERVUAR KAYAÇ ISLATIMLILIĞININ İNCE TABAKA YÜKSELME YÖNTEMİYLE ÖLÇÜLMESİ

ÖZET

Bu yüksek lisans laboratuar çalışmasında, minerolojik olarak heterojen kompozisyona sahip gözenekli madde ile temas halinde olan iki karışmayan akışkanın katı yüzeyi ile oluşturacakları kontak (temas) açısının ölçülebilirliği araştırılmıştır. Bu araştırmada, kontak açılarının dinamik hesaplanmasında kullanılan Washburn denklemi ve bu denklemin ince tabaka kılcal yükselme (thin layer wicking approach) yöntemine olan uygulaması açıklanmıştır.

Bu deneysel çalışmada, öğütülerek toz haline getirimiş numune "powder" olarak çeşitli kumtaşı ve kireçtaşı kayaç örnekleri ile bu kayaçları oluşturan temel saf mineraller (kuvars ve kalsit) kullanılmıştır. Çalışmada yükselme sıvısı olarak saf su, ağırlıkça %2' lik NaCl tuzlu su çözeltisi, gazyağı, mineral oil ve ham petrol kullanılmış ve bunların numunenin katı yüzeyinde oluşturdukları temas açıları ölçülmüştür. Bu araştırma projesinde, öğütülmüş mineraller (powder) üzerinde uygulanan ince tabaka kılcal yükselme tekniğinin heterojen yapıdaki kayaçların temas açılarının bulunmasında uygulanabilirliği ve ıslatımlılık ile temas açısı arasındaki ilişki araştırılmış ve sonuçları verilmiştir.

DETERMINATION OF RESERVOIR ROCK WETTABILITY BY THIN LAYER WICKING APPROACH

ABSTRACT

The present graduate research study is an attempt to investigate the possibility of contact angle determination of two immiscible fluids in contact with the solid surface of a porous material with heterogeneous mineralogical composition. Application of the Washburn equation for dynamic measurement of contact angle and the method of Thin Layer Wicking were described.

Experiments were conducted on the powdered samples of different sandstone and limestone rock samples and also their representative pure minerals such as quartz and calcite, respectively. In this study, distilled water, 2% NaCl brine, kerosene, mineral oil, and crude oil are used as a wicking liquid, and contact angles with respect to the solid sample's surface were measured. Applicability of the "Thin Layer Wicking Technique" for contact angle determination of the heterogeneous rock samples and the relation between the wettability and the contact angle were discussed.

1. INTRODUCTION

"Oil recovery from porous sedimentary rocks depends mainly on the overall efficiency with which oil is displaced by some other fluid. Interfacial phenomena in porous rocks lie at the heart of oil recovery because they determine the fraction of oil that moves from the swept region toward a producing well. Detailed studies of displacement efficiency from the pore spaces, commonly referred as microscopic displacement efficiency, were first reported over 70 years ago. Microscopic displacement efficiency is determined by the interactions of rock pore geometry and interface boundary conditions. These interactions constitute what is known as reservoir wettability" (Morrow, 1991).

Fluid distribution in porous media is affected not only by the forces at fluid/fluid interfaces but by the forces at fluid/solid interfaces (Green and Willhite, 1998). Wettability is an important phenomenon that controls the distribution, location, and flow of fluids in a reservoir. It has a strong influence on core analyses, such as dispersion, capillary pressure, waterflood behavior, relative permeability, tertiary recovery, irreducible water and oil saturation and electrical properties (Anderson, 1986). The wettability of a rock is related to the affinity of its surface for water and oil. For general definition, wettability is the relative preference of a solid surface to be coated by a certain fluid in a system (Morrow, 1991). Reservoir rocks have complicated pore structure and mineral composition, therefore measured wettability is the average wetting ability of the various minerals forming the rock surface.

In the past, petroleum reservoirs were considered to be strong water wet. Because before the migration of oil into the reservoir, it was thought that pore space was occupied with formation water. But in the beginning of 1940's it was seen that oil can wet the surface of sandstone (Bartell and Miller, 1928) and silica (Benner and Bartell, 1942). There are several methods for wettability measurements but mostly Amott, USBM (United States Bureau of Mines) and contact angle methods are preferred in the petroleum industry.

The first two methods can be used to measure average wettability of a rock where regular shaped cores are available. In addition, when pure fluids and artificial cores are used, contact angle is the best wettability measurement method (Anderson, 1986). The contact angle measures the wetting tendency of a liquid on a solid surface when another immiscible liquid is present (Hunter, 1987). If a small drop of a liquid is placed on a uniform, perfectly flat, solid surface, a contact angle is formed at the junction between three phases. If the contact angle is less than 90^o, liquid wets the solid surface and it is greater than 90^o, the drop rounds up and does not wet the surface. Additionally, the solid is said to have neutral or intermediate wettability if the contact angle is about 90^o. When the oil-water-rock system is considered, the system is defined as water wet if θ is between 0^o and 60^o to 75^o, the system is defined as oil wet if θ is between 180^o and 105^o to 120^o, in Figure 1.1 (Anderson, 1986). Some researchers use accurate boundaries for the separation of wettability types. For instance, Treiber et al. have chosen cut-off values of 75^o and 105^o whereas Morrow has chosen 62^o to 133^o or Chilingar and Yen use 80^o to 100^o (Morrow, 1991).

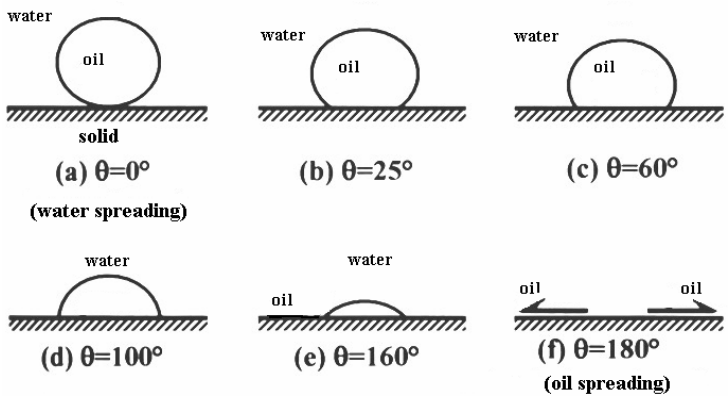

Figure 1.1 : Degrees of Wettability (Morrow, 1990)

a) Completely water wet b) Strongly water wet c) Water wet
d) Oil wet e) Strongly oil wet f) Completely oil wet

The terms intermediate (Marsden and Nikidas, 1962), fractional (Fatt and Klikoff, 1959; Iwankow, 1960) or heterogeneous (Browns and Fatt, 1956), mixed (Salathiel, 1973) and

speckled (Morrow et al., 1986) were introduced to indicate types of wetting conditions which are not simply either strongly water-wet or oil-wet (Jadhunandan, 1990; Gökmen, 2003). If the rock is strongly hydrophilic, the initial water wets the solid surface and occupies the small pores. If the rock is strongly oleophilic, the oil wets the solid surface and initial water is placed in the middle of the large pores as shown in Figure 1.2 (Cuiec, 1991).

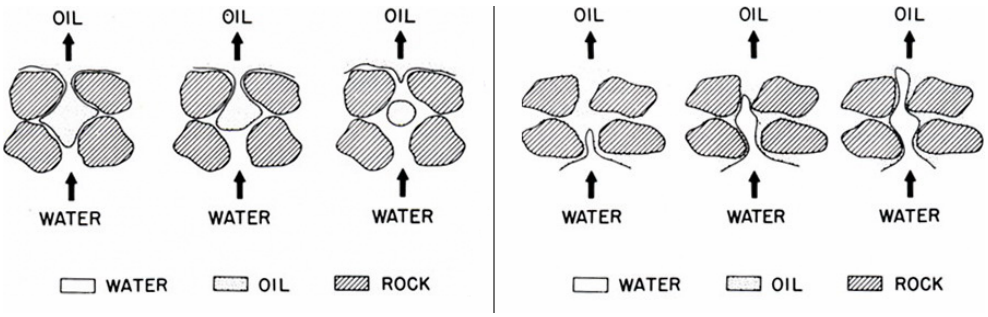

Figure 1.2 : Schematic Diagram of Water-Wet and Oil-Wet Rock (Morrow, 1991)

Contact angle defines the wetting behavior of solids or it can be said that it is a measure of surface hydrophobicity. As the contact angle increases, solid surface becomes more hydrophobic. Furthermore, it is also used to find the surface free energy of a solid. Surface energy components of solids are acknowledged as the key to realize the mechanism of surface-based phenomena. The energy of solid surfaces helps to predict most surface properties such as wetting, adsorption and adhesion. Therefore there is a strong relationship between wettability and measurements of contact angle and surface free energy components. A finite measurable contact angle can be obtained if γ_L is greater than γ_S and if γ_L is less than γ_S liquid spreads and wets the solid completely. Solids having higher surface free energies exhibit lower values of water contact angles that direct water wet surfaces (Yıldırım, 2001; Giese and van Oss, 2002). The elastic and viscous restraints of the bulk phase disable direct measurements of the surface tension components ($\gamma_S^{LW}, \gamma_S^+, \gamma_S^-$) and necessitate indirect methods (Schultz and Narin, 1992). Especially, contact angle measurements are utilized for determining the surface free

energy values of solids by measuring contact angles with at least three different liquids of which two must be polar and H-bonding (van Oss et al., 1988).

In some cases achieving a reproducible contact angle with direct contact angle measurements is not easy. For instance, contamination of the droplet by adsorption of impurities from the gas phase yields reduction of θ. Surface roughness can change θ value; when θ is smaller than 90^o roughness causes lessening, and when θ is greater than 90^o roughness causes increasing in θ value. Also hysteresis can be seen in contact angle measurements and creates differentiation between advancing and receding contact angle values (Rosen, 1989).

The measurement of contact angle on flat surfaces is useless when large samples of solid or flat and polished solid surfaces are unavailable. Pore geometry, surface roughness and adsorbility of porous surfaces prevent the direct measurements of contact angles. Also polishing the surface of solids causes atomic rearrangements and provides creation of new surfaces. Moreover, in contact angle visualization reservoir is modeled with pure and single mineral which limits the investigation of mineralogically heterogeneous rock system (Wolfram, 2002; Morrow, 1991), and flat, smooth and polished surface does not wholly represent the naturally porous surface of the rocks composed of several different minerals (Yıldız, 1998). In this situation, quantifying the wetting characteristics of solid surfaces with a capillary rise in a bed of particles is a better approach when contact angles cannot be directly measured. As a consequence, when the powdered form of a single mineral crystal or rock containing many different components exist, capillary rise and thin layer wicking methods are available for estimating the contact angle.

A liquid may penetrate spontaneously into a porous media by capillary forces. This process is referred to as wicking .Washburn (1921) formulated the rate of penetration of a liquid into a porous medium or powdered material. According to Washburn (1921), the distance penetrated by a liquid flowing under capillary pressure alone into a horizontal capillary is equal to $\sqrt{\frac{r\gamma\cos\theta}{2\mu}t}$. In the 1980s Van Oss developed Thin Layer Wicking method for measuring the contact angles of all minerals, even with irregularly shaped, such as nonswelling clays, talc, dolomite, limestone, calcite, silicates and the cuboids

hematite (Karagüzel et al., 2005). In this method, a thin layer of powdered solid sample is deposited on glass slide. This facilitates penetration of the liquid into the layer and a sharp visible progressing contact angle line can be seen. Using the wicking results, wetting contact angle can be calculated with the Washburn equation;

$$l^2 = \frac{t\, r\, \gamma_L \cos\theta}{2\mu} \qquad \textbf{(1.1)}$$

Where, l is the height of the column of liquid has reached by capillary rise in time t, r is the average radius of the pores of the porous medium, θ is the contact angle, γ_L is the surface tension and μ is the viscosity of the liquid. θ and r are the unknowns of the equations. In order to find these values, a low energy liquid that wets the surface completely is used, in this situation θ will be 0^o and r can be found. Contact angles of studied liquids can then be calculated (van Oss, 1994).

The Amott test and the USBM test are the most commonly used methods of quantifying wettability based on oil/brine/rock displacement behavior (Cuiec, 1990). Both depend on capillary pressure and microscopic displacement efficiency (Morrow, 1990). The serious weakness for USBM method is that the test does not recognize systems that achieve residual oil saturation by spontaneous imbibition (Ma et.al, 1994). In other words, the method does not recognize very strongly water wet or very strongly oil wet systems. On the other hand, the Amott test demonstrates the effect of displacement by capillary forces due to water or oil imbibition over total displacement forces of capillary and viscous together (Yıldız and Gökmen, 2001). A weakness of the Amott test is its failure to distinguish between important degrees of strong water-wetness (Morrow, 1990). This was the reason that in this study, application of the Washburn equation for dynamic determination of contact angle and the method of Thin Layer Wicking were described in order to qualitatively characterize wettability of porous material with heterogeneous mineralogical composition such as sandstones and carbonates.

The primary objective of the present study was to determine wettability of a rock composed of many different mineral constituents by applying Thin Layer Wicking approach.

2. LITERATURE REVIEW

2.1 Interfacial Tension

When two immiscible phases exist together, interface is the boundary formed between the phases. Interfaces can be classified according to state (solid, liquid or gaseous) of two adjacent phases. When a liquid is in contact with a gas, another immiscible fluid, or a solid, intermolecular attraction within the liquid is unbalanced at the interface. This excess energy exists at any interface. If one of the phases is the gas phase, the measurement is called surface tension, and if the interphase of two liquids is investigated, the measurement is called interfacial tension. It can be quantified as the force acting normal to the interface per unit length (force/unit length, mN/m). According to Defay and Prigogine (1966), interfacial tension is defined in terms of energy;

$$\sigma = G - \sum_{i} \Gamma_i \mu_i \qquad \textbf{(2.1)}$$

G is the Gibbs free energy per unit area; Γ_i is the adsorption of the element i in moles per unit area; and μ_i is the chemical potential of the element. Thus, the interfacial tension is equal to the free surface energy per unit area, G, if the system is in physical-chemical equilibrium, that is $\sum_{i} \Gamma_i \mu_i = 0$ (Francisca et al., 2003).

2.2 Contact Angle

The intersection region of solid-liquid, solid-fluid, and liquid-fluid is called the contact line where the contact angle is formed. The contact angle is an angle between the tangent to the liquid-fluid interface and the solid interface. Two contact angles can be defined; the intrinsic contact angle, θ, is the angle at a very short distance from the solid

and the apparent contact angle, θ_a, that is measured at the macroscopic level (Marmur, 1992).

In 1805, Thomas Young suggested treating the contact angle of a liquid as the result of the mechanical equilibrium of a drop resting on a plane solid surface under the action of three surface tensions; γ_{LV} at the interface of the liquid and vapor phases, γ_{SL} at the interface of the solid and the liquid, and γ_{SV} at the interface of the solid and vapor. (Zisman, 1944). In the presence of a vapor phase, if a non-reactive liquid does not wholly coat the solid surface, which is plane, undeformable, perfectly smooth and chemically homogeneous, the liquid surface will intersect the solid surface at a "contact angle" θ. The basic Young equation defines the contact angle as following form illustrated in Figure 2.1.

$$\cos\theta = \frac{\gamma_{SV} - \gamma_{SL}}{\gamma_{LV}} \qquad \textbf{(2.2)}$$

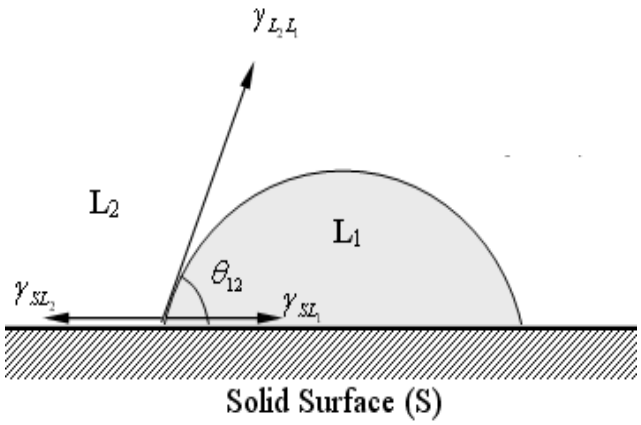

Figure 2.1 : Solid-Liquid-Vapor Interface

This equation can be derived by calculating the difference of the surface free energy F_s of the system caused by a small displacement δz of the *S/L/V* contact (triple line, *TL*) line under the assumptions given in Figure 2.2. The total length of *TL* is constant throughout its displacement, the radius *r* of the *TL* region is larger than the range of the atomic (or molecular) interactions in the system but must be smaller than the characteristic dimension of the liquid and inside the region of radius *r*, the intersection of the *L/V*

surface with the plane of figure is a straight line, the variation of interfacial free energy per unit length of *TL*, resulting from a small linear displacement δz of *TL* is:

$$F_s (z + \delta z) - F_s(z) = \delta F_s = (\gamma_{SL} - \gamma_{SV}) \delta z + \cos(\theta)\gamma_{LV} \delta z \quad \textbf{(2.3)}$$

The equilibrium condition $d(\delta F_s) / d(\delta z) = 0$ forms the classical equation of Young (Eustathopoulos et al., 1999).

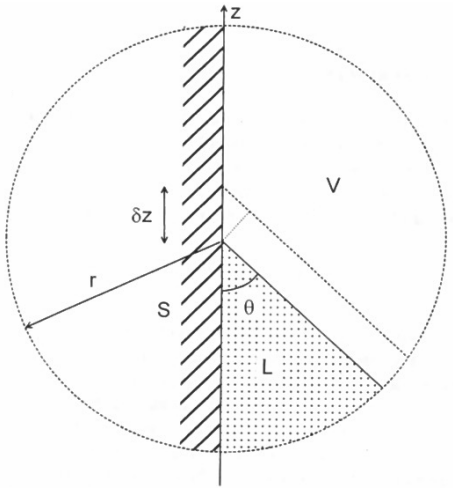

Figure 2.2 : Displacement of a Triple Line Around its Equilibrium Position That Allows Derivation of the Young Equation (Eustathopoulos et al., 1999).

Another approach established by Dupré demonstrates the relation between the reversible work of adhesion of liquid and solid, W_A, γ_{SV} and γ_{SL} :

$$W_A = \gamma_{SV} + \gamma_{LV} - \gamma_{SL} \quad \textbf{(2.4)}$$

This expression shows that the reversible work of separating the liquid and solid phases should be equal to the change in the free energy of the system.

According to Sumner (1937), the Young equation can also be derived thermodynamically for the ideal plane solid surface on condition that the system is in thermal and mechanical equilibrium so γ_{SL} ,γ_{SV} and γ_{LV} are defined as follows:

$$\gamma_{SL} = \left(\frac{\partial F}{\partial A_{SL}} \right)_{T,\mu_i} \quad (2.5)$$

$$\gamma_{SV} = \left(\frac{\partial F}{\partial A_{SV}} \right)_{T,\mu_i} \quad (2.6)$$

$$\gamma_{LV} = \left(\frac{\partial F}{\partial A_{LV}} \right)_{T,\mu_i} \quad (2.7)$$

Here; F is the Helmholtz free energy of the system, A, is the area of the interfaces, T is the temperature and μ_i is the potential of each component in the phases.

Surface wettability and hydrophobicity, surface free energy and its components, surface adsorption and heterogeneity can be determined by the contact angle estimations. The contact angle can be given in two forms; Static and Dynamic. After a drop of a liquid place over a solid surface, all phases (solid, liquid, and gas) try to reach their equilibrium position, as soon as the three phase line is not moving any longer; the static contact angle is achieved. On the other hand, while the liquid is spreading over the solid and the three phase line is in controlled motion, the contact angle changes continuously with time and dynamic contact angle can be measured.

2.2.1 Contact Angle Measurements in Liquids

Young's equation can be used to find contact angles of a drop of a liquid, L on a solid, S, immersed in a different liquid. If the two liquids are immiscible, then we can define the following equation;

$$\gamma_{SL_2} = \gamma_{L_1L_2} \cos\theta_{SL_1} + \gamma_{SL_1} \quad \textbf{(2.8)}$$

where, γ_{SL_1}, γ_{SL_2}, and $\gamma_{L_2L_1}$ are solid surface interfacial energies for a given liquid and the interfacial tension between two immiscible liquids, respectively, and θ_{SL1} is a contact angle (van Oss 1994; Adamson 1990). Here, the difference of solid interfacial energies on the left hand side of above equation is called adhesion tension and is usually referred as the difference between the solid surface interfacial tensions of non-wetting and wetting phases. If adhesion tensions of both liquids measured in one vapor environment

are known, the contact angle on liquid-liquid-solid interface then can be easily calculated (Tacibayev, 2005),

$$cos\theta_{12} = \frac{\left(\gamma_{SL_2} - \gamma_{SL_1}\right)}{\gamma_{L_2L_1}} = \frac{\left(\gamma_S - \gamma_{SL_1}\right) - \left(\gamma_S - \gamma_{SL_2}\right)}{\gamma_{L_2L_1}}$$

$$= \frac{\gamma_{L_1} cos\theta_1 - \gamma_{L_2} cos\theta_2}{\gamma_{L_2L_1}} \qquad \textbf{(2.9)}$$

2.2.2 Contact Angle on Heterogeneous Surfaces- Cassie's Equation

In 1948, Cassie gave a formula for contact angles on solid surfaces composed of different materials;

$$\cos\theta_A = f_1 \cos\theta_1 + f_2 \cos\theta_2 \qquad \textbf{(2.10)}$$

θ_A aggregates contact angle measured on the heterogeneous surface. *f's* are the proportions of the surface occupied by materials and $f_1 + f_2 = 1$. θ_1 and θ_2 are the contact angles found on solid surface only consisting of material 1 and 2 respectively (Giese et al., 2002; van Oss, 1994).

2.2.3 Limitations of Contact Angle Measurements

2.2.3.1 Hysteresis

In contact angle measurements an important problem, which is called hysteresis, occurs. In reality, solid surfaces are non-ideal and don't satisfy the conditions of Young's equation to be valid, thus a liquid drop on a surface can have many different stable contact angle (Anderson, 1986). The angle measured just after a drop of liquid has advanced on the solid surface is called advancing angle *(θ_A)*, and the angle measured just after arrest of a liquid drop is called receding angle (θ_R) shown in Figure 2.3 (Schultz and Narin, 1992). The difference between the maximum (advancing) and minimum (receding) contact angle values is called the contact angle hysteresis.

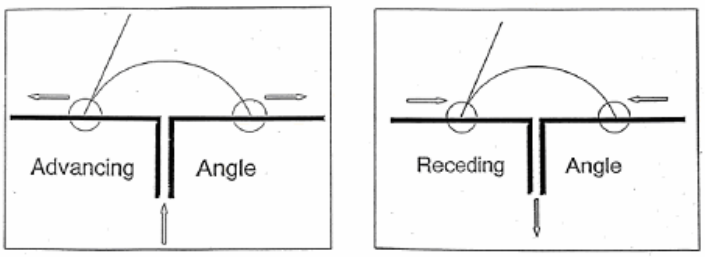

Figure 2.3 : Illustrations of Advancing and Receding Contact Angles

According to Adamson (1990), there are three main reasons for hysteresis. First one, which raises the hysteresis, is the contamination of liquid or solid surface. Second, hysteresis effects are associated with rough surfaces. The surface roughness causes many metastable states of the drop to be formed with different contact angles and the macroscopically and microscopically observed contact angles will not be the same. The third cause is the surface immobility on a macromolecular scale. The contact angle cannot reach its equilibrium value because surface immobility creates hysteresis by resisting the fluid motion (Anderson, 1986). There is another very important phenomenon in hysteresis called the surface heterogeneity and it is tried to be avoided by measuring the angle on a single mineral crystal, where as a core contains many different constituents. Also for wetting of polymers, Schultz and Nardin's (1992) experiments shows that hysteresis are related with the polar character of the polymer surface and reorientation of polar groups on the surface in contact with a polar liquid such as water. Timmons and Zisman (1966) informed that an apparent penetration of water molecules into a surface could cause a significant contact angle hysteresis.

2.2.3.2 Spreading Pressure

In Young's equation, γ_{sv} is assumed to be to equal to γ_s^0 . First one describes the surface of a solid in equilibrium with the vapor of a liquid and the latter, γ_s^0, a solid in equilibrium with its own vapor. Consequently, in some cases they have distinction caused by adsorption. The adsorption of the vapors of the wetting liquid onto the solid surface can reduce the surface energy of the solid (Hiemenz and Rajagopalan, 1997). This is defined by spreading pressure, $\Pi_e = \gamma_s^0 - \gamma_{sv}$, having the dimensions of an

energy per unit area or a force per unit length (Hunter, 1993). This term should be added to Young's equation;

$$\gamma_L \cos\theta = \gamma_S - \gamma_{SL} + \Pi_e \quad \textbf{(2.11)}$$

However, under non-spreading conditions there is no need to add imaginary equilibrium spreading pressure. This can be neglected based on the results of wicking and thin layer wicking that state with non spreading liquids (i.e. $\gamma_L > \gamma_S$ and $\cos\theta < 1$) neither spreading nor pre-wetting takes place, as evidenced by a strongly negative slope of plots of $\mu l^2/t$ vs. γ_L (van Oss, 1994).

2.3 Theory of Wetting

On the basis of thermodynamic wetting can be defined by the physicochemical reaction caused by intermolecular forces of attraction. Wettability represents the energy lost by the system during the wetting of a solid by a liquid. This can be shown with

$$\gamma_m = -(\frac{\partial G}{\partial s})_{T,P} \quad \textbf{(2.12)}$$

where, *G* is the free Gibbs energy, *T* is the temperature, *P* is the pressure and s is the surface of the solid. If $(\partial G/\partial s)_{T,P} < 0$, the reaction is spontaneous and wettability is positive (Morrow, 1991).

Wettability is defined as the tendency of one fluid to spread on or adhere to a solid surface in the presence of other immiscible fluids seen in Figure 2.4 (Anderson, 1986). According to Adamson (1990), wetting indicates that the contact angle between a liquid and a solid surface is zero or so close to zero that the liquid spreads over the solid easily. Young described the contact angle as:

$$\gamma_L \cos\theta = \gamma_S - \gamma_{SL} \quad \textbf{(2.13)}$$

The reversible free energy of adhesion ΔG_{SL} of the liquid on the solid (also called solid-liquid interfacial free energy) was given by Dupré (1869) as:

$$\Delta G_{SL} = \gamma_{SL} - \gamma_S - \gamma_L \quad \textbf{(2.14)}$$

by combining Young's and Dupré's equation, Harkins & Feldman's spreading coefficient that determines the ability of the liquid to wet a solid can be found.

$$S = \Delta G_{LL} - \Delta G_{SL} \quad \textbf{(2.15)}$$

ΔG_{LL} is the free energy of cohesion of the liquid and equals to -2 γ_L, then;

$$S = \gamma_S - \gamma_L - \gamma_{SL} \quad \textbf{(2.16)}$$

$$S = -\gamma_L (1 - \cos\theta) \quad \textbf{(2.17)}$$

For nonspreading condition $S \leq 0$ and for spreading condition $S > 0$ referring that the liquid wets the solid surface (Zisman, 1944). The difference between the work of adhesion and the work of cohesion (W_A-W_C) gives the spreading coefficient, where W_C is equal to $2\gamma_{LV}$. A positive spreading coefficient is necessary for a liquid to spread on a solid surface seen in Figure 2.6. Therefore, wettability can be estimated from calculating the surface tension of the solid or solid-liquid interfacial free energy and from measurements of the contact angle (Michel et al., 2001).

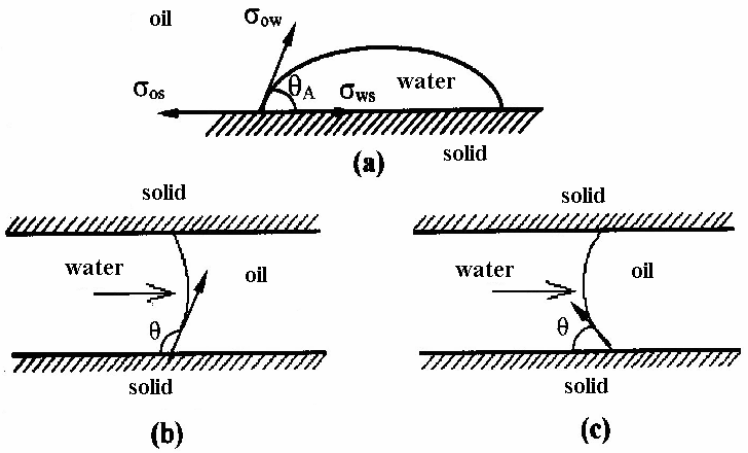

Figure 2.4: Schematic representation of wetted rocks (Gökmen, 2003)
a) wettability of a rock b) oil-wet c)water-wet rock

There appear many different methods for wettability measurements. They are divided into two; quantitative methods: contact angles, Amott (imbibition and forced displacement) and USBM wettability method; qualitative methods: imbibition rates, microscope examination, flotation, glass slide method, relative permeability curves, capillarimetric method, displacement capillary pressure, reservoir logs, nuclear magnetic resonance, and dye adsorption (Adamson, 1986).

The Amott test (Amott, 1959) and the USBM test (Donaldson et al., 1969) are the most commonly used methods of quantifying wettability based on oil/brine/rock displacement behavior (Cuiec, 1990). Both depend on capillary pressure and microscopic displacement efficiency. The Amott test for characterizing wettability is based on imbibition and forced displacement. The main principle of this method is that the wetting fluid generally imbibes spontaneously into the core, displacing the non-wetting one (Anderson, 1986). Method consists of two parts after establishing the S_{wi}. The first part is spontaneous imbibition in water followed by forced displacement by water. The second part is a test for spontaneous imbibition in oil at a residual oil saturation followed by forced displacement by oil (Yıldız and Gökmen, 2001). The test results are expressed with Amott wettability indices. The ratio of the spontaneous increase in water saturation the total increase is the wettability index to water, I_w. The ratio of oil imbibed spontaneously to the total displacement of oil give the wettability index to oil, I_o. The difference between I_w and Io gives the Amott-Harvey wettability index (Morrow and Mason, 2001; Zhou et al., 1996). The imbibition can take several hours to more than 2 months to complete. If the imbibition is stopped after a short period of time underestimation of Io and I_w can be occurred. Also the main weakness of the Amott test is that it is insensitive near neutral wettability (Anderson, 1986). Moreover, it is failure to distinguish between important degrees of strong water-wetness (Morrow, 1990).

US Bureau of Mines (USBM) has developed a quantitative method for determining the average wettability of porous media that contains brine and crude oil by using capillary pressure curves determined with a centrifuge (Donaldson et al., 1969). This method is based on correlation between the degree of wetting and the areas under the capillary-pressure curves as seen in the Figure 2.5 (Robin, 2001).

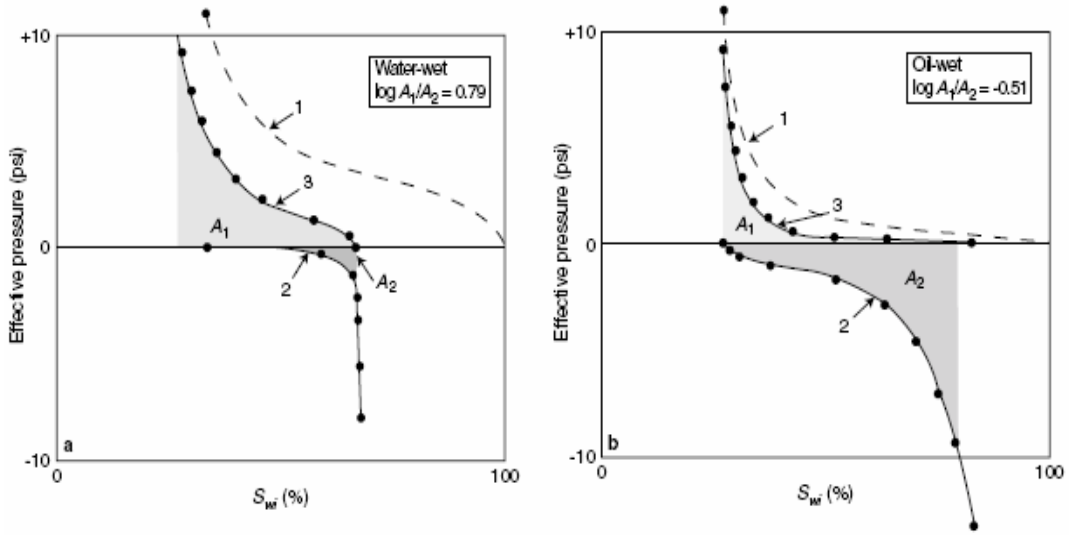

a) Water Wet b) Oil Wet

Figure 2. 5 : Capillary Pressure vs. Saturation Curves (Robin, 2001)

A_1 and A_2 are the areas under the capillary pressure versus saturation curves obtained during oil and brine drives respectively (Anderson, 1986). These areas are representative of the energy needed to inject either fluid in the porous medium. When $A_1>A_2$ the solids are preferentially water-wet, on the other hand, when $A_2>A_1$ the solids are preferentially oil-wet. The main advantage over the Amott test is its sensitivity near neutral wettability (Anderson, 1986). The serious weakness for USBM method is that the test does not recognize systems that achieve residual oil saturation by spontaneous imbibition[8]. In other words, the method does not recognize the very strongly water wet or very strongly oil wet systems (Ma et. al, 1994; Yıldız and Gökmen, 2001). In addition, USBM test cannot determine whether a system has fractional or mixed wettability while Amott sometimes sensitive. Furthermore; USBM has a minor disadvantage, sample must be spun in centrifuge so it can be measured on plug size samples (Anderson, 1986).

2.3.1. Types of Wetting

Osterhuf (1930) has given three types of wetting:

2.3.1.1. Adhesive wetting-the Young- Dupré equation

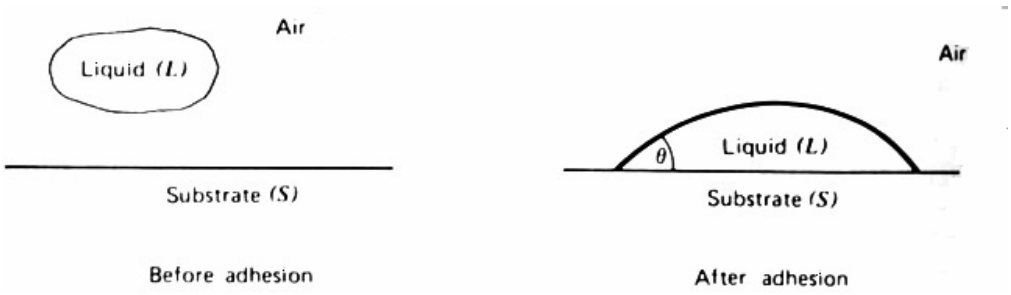

Figure 2.6 : Adhesional Wetting (Rosen, 1989)

In adhesional wetting in Figure 2.6, a liquid that is not in touch with a substrate makes contact with that substrate and adheres to it. When the solid surface is lowered towards the liquid until contact is established, the change of interfacial free energy of the system, or the work gained, is given by:

$$-W_A^o = \gamma_{SL} - (\gamma_{SV}-\gamma_{LV}) \quad \textbf{(2.18)}$$

Here $-W_A^o$ equals to work of adhesion of the liquid phase on the solid. So Young-Dupré equation is;

$$\cos\theta = \frac{W_a^0}{\gamma_{LV}} - 1 \quad \textbf{(2.19)}$$

In this equation, cohesion forces create γ_{LV} and adhesion forces create W_A^o (Eustathopoulos et al., 1999). The difference between the work of adhesion and cohesion equals to spreading coefficient $S_{L/S;}$

$$W_a - W_C = \gamma_{SV} - \gamma_{SL} + \gamma_{LV} - 2\gamma_{LV} \quad (2.20)$$

$$S_{L/S} = \gamma_{SV} - \gamma_{SL} - \gamma_{LV} \quad (2.21)$$

When these works are equal we get:

$$\gamma_{SV} - \gamma_{SL} + \gamma_{LV} = 2\gamma_{LV} \quad (2.22)$$

$$\gamma_{LV}(\cos\theta + 1) = 2\gamma_{LV} \quad (2.23)$$

Here, if θ= 0 then cos θ=1 and $S_{L/S} = 0$. Therefore, if Wa >Wc the liquid spreads over the substrate to form a thin film (Rosen, 1989). The driving force of this kind of wetting is simply expressed as; $\gamma_{SV} + \gamma_{LV} - \gamma_{SL} = 0$.

2.3.1.2 Equilibrium and non-equilibrium work of adhesion - work of spreading

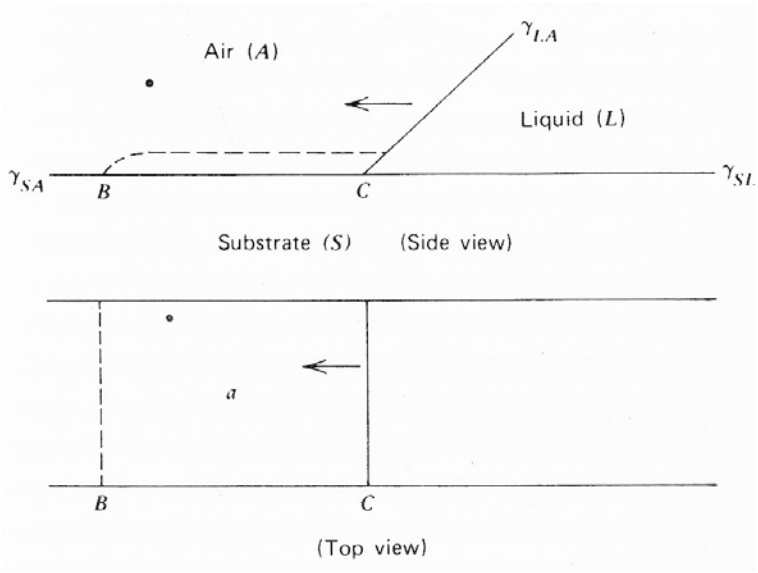

Figure 2.7 : Spreading Wetting (Rosen, 1989)

When a liquid in contact with a substrate spreads over and displaces another fluid, this is called spreading wetting seen in Figure 2.7 (Rosen, 1989). Surface energy reduction ($\Delta\gamma_{SV}$) occurs when there is adsorption of liquid vapors on the solid surface. γ_{SV} and W_a are denoted (P_{sat}) and $W_a(P_{sat})$ when the solid surface is in equilibrium with a saturated vapor of the liquid at a partial pressure of Psat.

$$\gamma^{0}_{SV} = \gamma_{SV}(P_{sat}) + \Delta\gamma_{SV}(P_{sat}) \quad (2.24)$$

$$W^{0}_{a} = W_a(P_{sat}) + \Delta\gamma_{SV}(P_{sat}) = \gamma_{LV}(1 + \cos\theta) + \Delta\gamma_{SV}(P_{sat}) \quad (2.25)$$

Formation of a continuous liquid film on a solid surface causes the change in the interfacial energy of the system. This can be represented with the work of spreading, $W_s(P_{sat})$ (Eustathopoulos et al., 1999) ;

$$W_s(P_{sat}) = \gamma_{LV} + \gamma_{SL} + \gamma_{SV}(P_{sat}) = 2\gamma_{LV} - Wa(P_{sat}) \quad \textbf{(2.26)}$$

To summarize, the driving force is equal to $\gamma_{SV} - (\gamma_{SL} + \gamma_{LV})$ and this is named as spreading coefficient $S_{L/S}$. If spreading coefficient is positive liquid will spread over the substrate, and if it is negative, spreading cannot occur spontaneously.

2.3.1.3 Immersion

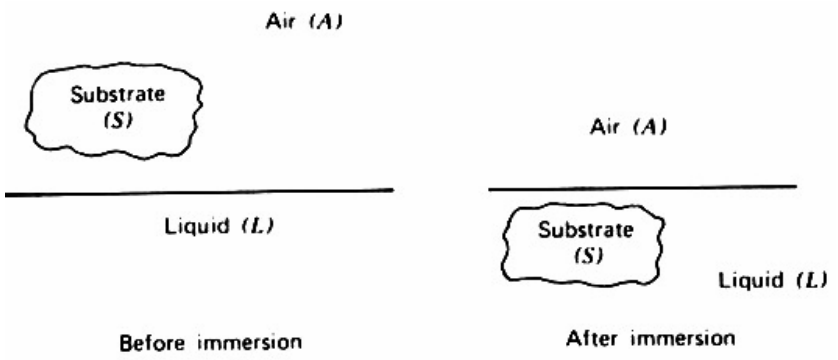

Figure 2.8 : Immersional Wetting (Rosen ,1989)

In immersional wetting in Figure 2.8, substrate which is not in contact with a liquid is immersed by the liquid totally. The driving force of this wetting phenomenon is the quantity of; $\gamma_{SV} - \gamma_{LV}$ (Rosen, 1989). Work of immersion, W_i, defines the surface energy change when a S/V surface of unit area is replaced by a S/L interface of equal area by immersion of a solid in a liquid.

$$Z_e = \frac{2(\gamma_{SL} - \gamma_{SV})}{r\rho g} \quad \textbf{(2.27)}$$

Where Z_e is the depression of the liquid in the capillary, r is the internal radius of capillary. The thermodynamic quantity ($\gamma_{SL} - \gamma_{SV}$) is the work of immersion that

describes any infiltration process of liquids into porous media (Eustathopoulos et al., 1999).

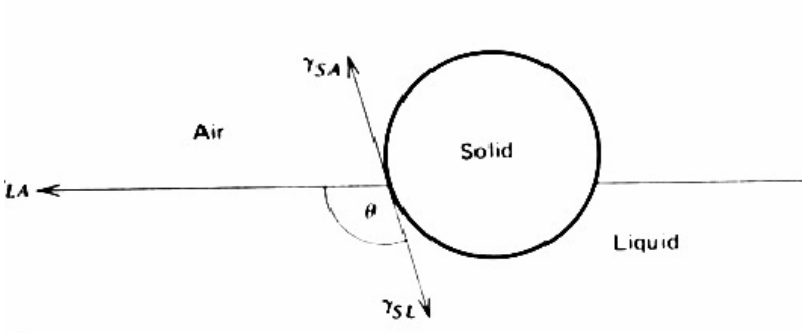

Figure 2.9 : Contact Angle of Partially Immersed Solid (Rosen, 1998)

The depth of immersion of the solid on the wetting liquid can be found by the contact angle, when the contact angle decreases, the dept of immersion increases (Figure 2.9). Therefore, immersion is complete when $\theta = 0^{o}$.

2.4 Capillary Pressure

If two immiscible fluids are in contact in a porous medium, a meniscus is formed between these two fluids. The pressure difference between wetting and nonwetting phase across the interface is the capillary pressure (Yildiz, 1998). Along with force balances, capillary pressure can be defined:

$$\sum \vec{F}_x = 0 \qquad (2.28)$$

$$P_{nw}(\pi r^2) - \gamma_{nw,s}(2\pi r) - P_w(\pi r^2) + \gamma_{w,s}(2\pi r) = 0 \qquad (2.29)$$

$$\pi r^2 (P_{nw} - P_w) = 2\pi r(\gamma_{nw,s} - \gamma_{w,s}) \qquad (2.30)$$

$$P_{nw} - P_w = \frac{2(\gamma_{nw,s} - \gamma_{w,s})}{r} \qquad (2.31)$$

$$P_c = P_{nw} - P_w = \frac{2\gamma_{w,nw}\cos\theta}{r} \qquad (2.32)$$

where, P_{nw} and P_w are pressure difference across the nonwetting and wetting phase respectively, r is the radius of the capillary, $\gamma_{w,s}$ is the surface tension of wetting phase (dyne/cm), $\gamma_{nw,s}$ is the surface tension of nonwetting phase (dyne/cm), and $\gamma_{w,nw}$ is the interfacial surface tension of wetting/nonwetting phase (dyne/cm). According to this equation, capillary pressure is associated with interfacial tension, capillary radius and which defines the relative wettability characteristics of the fluids on solid surface. The phase that has lower capillary pressure will preferentially wet the porous medium (Green and Willhite, 1998).

2.4.1 Capillary Rise and Washburn Equation

When a powdered solid is in interest, the mechanism of the wetting is related with the capillary rise phenomenon (Adamson, 1990). The difference between the solid-air and solid-liquid interfacial energies is the driving force (adhesion tension) for a liquid into a powder bed in a capillary. There occurs a pressure difference across the curved liquid-vapor interface and this difference is given in terms of interfacial energies by;

$$\Delta P = \frac{2(\gamma_S - \gamma_{SL})}{r} \qquad \textbf{(2.33)}$$

The Young equation (2.13) can be utilized, if the liquid's contact angle on the solid is larger than zero, consequently pressure difference at the interface boundary can be defined as the liquid surface tension and contact angle;

$$\Delta P = \frac{2(\gamma_L \cos\theta)}{r} \qquad \textbf{(2.34)}$$

The voluminal laminar stationary flow, Φ_V, of incompressible uniform viscous liquid through a capillary with the constant circular cross-section can be modelled as in the following Figure 2.10. and flow rate is calculated from Hagen-Poiseuille equation:

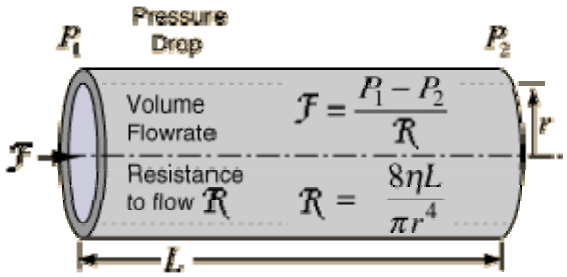

Figure 2.10: Capillary With the Constant Circular Cross-Section

$$\Phi_v = \frac{dV}{dt} = \upsilon_s \pi r^2 = \frac{\pi r^4}{8\mu}\left(-\frac{dP}{dz}\right) = \frac{\pi r^4}{8\mu}\frac{\Delta P}{L} \qquad \textbf{(2.35)}$$

here, dV is the volume of the liquid that penetrates through cross section of a capillar in time dt, and equals to $\pi r^2 dl$. Thus we can write the expression for the velocity under laminar conditions:

$$\frac{dl}{dt} = \frac{r^2 \Delta P}{8\mu l} \qquad \textbf{(2.36)}$$

substituting pressure difference that was given in equation (2.34) into above equation:

$$\frac{dl}{dt} = \frac{r\gamma\cos\theta}{4\mu l} \qquad \textbf{(2.37)}$$

and integrating this equation with the initial condition of l=0 at t=0; we obtain the Washburn equation.

$$l^2 = \frac{r\gamma\cos\theta}{2\mu}t \qquad \textbf{(2.38)}$$

where r is the average radius of the capillary, γ is the surface tension and μ is the viscosity of the liquid. The $\gamma\cos\theta/2\mu$ term is defined as the coefficient of penetrance or the penetrativity of the liquid and measures the penetrating degree of a liquid (Washburn, 1921; Yıldırım, 2001).

The Washburn Equation can be used to calculate contact angle of powders or porous solids. Capillary rise velocity of a liquid in capillary tube filled with packed solid powder provides determination of the contact angle value of that imbibing liquid (Giese et al., 2002; Yıldırım, 2001). This equation assumes that the liquid penetrates into a capillary filled with air or vapor having negligible viscosity (Marmur, 1992).

2.4.2 Thin Layer Wicking

The capillary rise method is limited due to the requirement of well-packed columns of monodisperse particles. Instead of capillary rise technique, Van Oss has developed an alternative method for determining the contact angles of powdered solids (Van Oss, 1994; Yıldırım,2001). This method, which was first suggested by Chaudhury, is known as Thin Layer Wicking and it also depends on Washburn equation (Giese et al., 2002). When powdered particles are in question it is hard to define their radius. If they are treated as a bundle of capillaries with varying radii, it can then be found a representative r value which is called effective radius, r^*. For the determination of r^*, we have to use completely wetting non-polar liquids having low energy. In such a case, it can considered that $\cos\theta$ in Washburn equation equals to 1. With these approaches, the wicking experiment is accomplished by preparing an aqueous suspension of powder and spreading it over a microscope slide. After drying the sample, coated glass slide is immersed into the liquid. The velocity of the liquid is measured in terms of the length, l, is traveled by a liquid in time, t. First experiment should be done with a spreading n-alkane liquid (standard liquid) in order to find r^*. The plot of l^2 versus t gives a straight line with a slope that is needed in modified Washburn equation (2.39):

$$r^* = \frac{2\mu}{\gamma}\frac{l^2}{t} \qquad \textbf{(2.39)}$$

If a second wicking experiment with the liquid in question (test liquid) is applied, the advancing contact angle value of powdered solid can be calculated with the Washburn equation by the help of r^*:

$$\theta = \cos^{-1}\left(\frac{2\mu}{r^{*}\gamma}\frac{l^{2}}{t}\right) \quad \textbf{(2.40)}$$

The main advantage of the TLW method is, its suitability for polydispersed suspensions of irregularly shaped particles (Yıldırım, 2001). Semi flat shaped particles do not create homogeneous settlement in capillary tube. On the other hand, they do more homogeneous packing during thin layer settling over glass slide because they settle their large surface and form homogeneous bed of powder. This enables the reproducibility and repetability of the test results (Karagüzel, 2005).

2.5 Surface Free Energy

The surface free energy of solids is a characteristic parameter in determination of the surface properties like wetting, spreading, adhesion, and adsorption. Surface free energy is defined as the work required increasing the area of substance by one unit area. It is quantified in terms of the forces acting on a unit length at the solid-liquid interface. It is also referred as the surface tension of the solid because the units' force/length and energy/area are the same (N/m), but the physical functions are different. According to Adam (1956), the surface tension is numerically equivalent to the surface energy for all pure liquid and nonstressed pure solid surfaces.

Solid surfaces are divided into high and low energy surfaces. Solids that have high specific surface free energy have high energy surfaces. Their atoms are held together by the chemical bonds; therefore large input of energy is needed to fracture these solids. These energies are ranging from 1000 to 4000 mJ/m^2. On the contrary, solids that have low specific surface free energies have low energy surfaces, and their molecules are held by physical forces, especially van der Waals. The free energy of these surfaces are smaller than 100 mJ/m^2 (Schrader, 1992).

According to Fowkes (1972), the surface tension of non-polar liquid or the surface free energy of non-polar solid are composed of;

$$\gamma = \gamma^{d} + \gamma^{i} + \gamma^{p} + \gamma^{h} + \gamma^{\pi} + \gamma^{ad} + \gamma^{e} \quad \textbf{(2.41)}$$

where, γ is the surface free energy of solids and indexes are referred to dispersion, induced dipole-dipole, dipole-dipole, hydrogen bonding, π bonding, electrostatic, acceptor-donor interaction, respectively.

Basically, this equation can be written with dispersion and nondispersion components;

$$\gamma = \gamma^{d} + \gamma^{n} \quad \textbf{(2.42)}$$

According to van Oss and co-workers, dispersion, induction and polarization terms can be combined into the Lifshitz van der Waals components,

$$\gamma^{LW} = \gamma^{d} + \gamma^{i} + \gamma^{p} \quad \textbf{(2.43)}$$

so the total surface free energy of solid and liquid surface tension equals to;

$$\gamma = \gamma^{LW} + \gamma^{AB} \quad \textbf{(2.44)}$$

where, $\gamma^{AB} = 2\sqrt{\gamma^{+}\gamma^{-}}$ and γ^{+} is the nonadditive part of the solid surface free energy resulting from electron acceptor interactions whereas γ^{-} results from electron donor interactions (Janczuk et al.,1998).

A solid phase is very different from a liquid phase because of the absence of surface mobility. For this reason, as in the case for a liquid phase, surface tension of a solid phase cannot be measured directly. Therefore, several different approaches have been used to measure solid surface energy, including direct force measurement, contact angle, sedimentation of particles, solidification front interactions with particles, film flotation, gradient theory, the Lifshitz theory of van der Waals forces, and theory of molecular interactions. Among these techniques, contact angle approach is the simplest one (Kwok et al., 2000). Besides, for the measurement of surface energy of powdered solids it is the most appropriate method. There are four basic approaches for evaluation of contact angles and they all depend on the Young's equation, $\gamma_{L}\cos\theta = \gamma_{S} - \gamma_{SL}$, that describes the wetting of solid surface with a liquid (Karagüzel, 2005).

2.5.1 Zisman Method (Critical Surface Tension)

Zisman et al. (1950) characterized the low surface energy surface by establishing a linear relationship between cosθ of non-polar liquids and their surface tension, γ_{LV}. If cosθ is plotted against γ_{LV}, a curve that can be extrapolated to cosθ = 1 is formed. The extrapolated value is called the critical surface tension of the solid and can be used to characterize the solid surface. It is the highest value of the surface tension of a liquid which will completely wet the solid surface (Giese et al., 2002; Schultz and Nardin, 1992). The energy of the solid surface can be calculated from the slope (m) of the line using the following formula (Karagüzel, 2005);

$$\cos\theta = 1 - m(\gamma_L - \gamma_S) \quad \textbf{(2.45)}$$

2.5.2 Fowkes Method (Geometric Mean)

Fowkes theory is based on two assumptions;

a. Surface energies are additive : $\gamma = \gamma^d + \gamma^p + \ldots$

b. Geometric mean is used for the work of adhesion for each type of energy:

$$W_{12}^d = 2\sqrt{\gamma_1^d}\gamma_2^d \ , \ W_{12}^p = 2\sqrt{\gamma_1^p}\gamma_2^p \quad \textbf{(2.46)}$$

This method examines the solid energy by dividing it into two components. Geometric mean approach combines the dispersive (γ^d) and polar (γ^p) components with the Young equation;

$$\gamma_L(1+\cos\theta) = 2(\sqrt{\gamma_L^d\gamma_S^d} + \sqrt{\gamma_L^p\gamma_S^p}) \quad \textbf{(2.47)}$$

Owens and Wendt (1969) rearranged the equation;

$$\frac{\gamma_L(1+\cos\theta)}{\sqrt{\gamma_L^d}} = \sqrt{\gamma_S^p}\left(\frac{\sqrt{\gamma_L^p}}{\sqrt{\gamma_L^d}}\right) + \sqrt{\gamma_S^d} \quad \textbf{(2.48)}$$

When the graph of $\sqrt{\gamma_L^p}/\sqrt{\gamma_L^d}$ versus $\gamma_L(1+\cos\theta)\sqrt{\gamma_L^d}$ is plotted, the slope will be $\sqrt{\gamma_S^p}$ and $\sqrt{\gamma_S^d}$ is the intercept. Then the total free surface energy is equal to $\gamma_S = \sqrt{\gamma_S^d} + \sqrt{\gamma_S^p}$.

2.5.3 Wu Method (Harmonic Mean)

Wu (1971) has claimed that the harmonic mean is better suited for low energy surfaces, such as polymer. In this method, harmonic means of polar and dispersive energy components are being used. Contact angle is found using the two liquids with known values of γ^d and γ^p. The values are put into the following equation, and two equations are solved for γ_S^d and γ_S^p (Karagüzel, 2005);

$$(1+\cos\theta)\gamma_L = 4\left(\frac{\gamma_L^d\gamma_S^d}{\gamma_L^d} + \gamma_s^d + \frac{\gamma_L^d\gamma_S^d}{\gamma_L^d} + \gamma_s^d\right) \quad \textbf{(2.49)}$$

2.5.4 Van Oss (Acid Base) Method

In this approach, contact angles against at least three liquids with known values of dispersive *(γ^d),* acid *(γ^+)* and base *(γ^-)* components are measured and put into the following equation:

$$0.5(1+\cos\theta)\gamma_L = \sqrt{\gamma_S^d\gamma_L^d} + \sqrt{\gamma_S^-\gamma_L^+} + \sqrt{\gamma_S^+\gamma_L^-} \quad \textbf{(2.50)}$$

and the total surface energy of the solid is;

$$\gamma_S = \gamma_S^d + \gamma_S^{AB} \quad \textbf{(2.51)}$$

$$\gamma_S^{AB} = 2\sqrt{\gamma_S^+\gamma_S^-} \quad \textbf{(2.52)}$$

2.5.4.1 Oss-Chaudary-Good Equation

OCG equation represents a thermodynamic approach to determining the values of the surface free energy components of solids and provides the calculation of surface free energies of powdered minerals with the help of contact angle values. From the studies of Fowkes et.al and Van Oss et.al, the surface free energy of a phase *i* can be written as;

$$\gamma_i = \gamma_i^{LW} + \gamma_i^{AB} \quad \textbf{(2.53)}$$

γ_i^{LW} is the non-polar components of surface free energy, while the γ_i^{AB} is the polar(acid-base) components and it conforms to the equation $\gamma^{AB} = 2\sqrt{\gamma^+\gamma^-}$ where γ^+ and γ^- are the non additive parts of the liquid surface tension or solid surface free energy resulting from electron acceptor and electron donor interactions (Yıldırım, 2001). Interaction between solid-liquid is explained with the following equation:

$$\Delta G_{SL} = \Delta G_{SL}^{LW} + \Delta G_{SL}^{AB} \quad \textbf{(2.54)}$$

for LW bonds Fowkes has proposed;

$$\Delta G_{SL}^{LW} = -2\sqrt{\gamma_S^{LW}\gamma_L^{LW}} \quad \textbf{(2.55)}$$

and for acid-base interactions Van-Oss has proposed;

$$\Delta G_{SL}^{AB} = -2\sqrt{\gamma_S^+\gamma_L^-} - 2\sqrt{\gamma_S^-\gamma_L^+} \quad \textbf{(2.56)}$$

If we combine these three equations we get,

$$\Delta G_{SL} = -2\sqrt{\gamma_S^{LW}\gamma_L^{LW}} - 2\sqrt{\gamma_S^+\gamma_L^-} - 2\sqrt{\gamma_S^-\gamma_L^+} \quad \textbf{(2.57)}$$

Dupré expressed the variation in free energy associated with the solid liquid interaction with the following relation:

$$\Delta G_{SL} = \gamma_{SL} - \gamma_S - \gamma_L \quad \textbf{(2.58)}$$

Substituting equation 2.58 into 2.57

$$\gamma_{SL} = \gamma_S + \gamma_L - 2(\sqrt{\gamma_S^{LW}\gamma_L^{LW}} + \sqrt{\gamma_S^+\gamma_L^-} + \sqrt{\gamma_S^-\gamma_L^+}) \quad \textbf{(2.59)}$$

work of adhesion or Gibbs free energy of interaction can be related to the interfacial energies through Young's equation;

$$\gamma_L \cos\theta = \gamma_S - \gamma_{SL} \quad \textbf{(2.60)}$$

by combining this equation with the Young's equation we get;

$$\gamma_L(\cos\theta+1)=2(\sqrt{\gamma_S^{LW}\gamma_L^{LW}}+\sqrt{\gamma_S^{+}\gamma_L^{-}}+\sqrt{\gamma_S^{-}\gamma_L^{+}}) \quad \textbf{(2.61)}$$

This is known as Van Oss- Chaudary-Good equation and characterizes a solid surface in terms of its surface free energy components as shown in Figure 2.11. (van Oss, 1994).

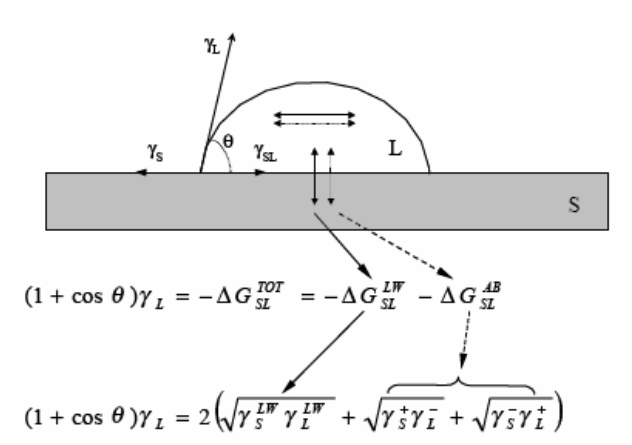

Figure 2.11 : Schematic Representation of the Contact Angle Formed Between a Liquid Drop and Solid Surface (Yıldırım, 2001)

For finding the value of γ_S, contact angle determination with three or more liquids which at least two must be polar should be done. If the contact angle of apolar liquid is measured, this equation is reduced to;

$$\gamma_L(\cos\theta+1)=2\sqrt{\gamma_S^{LW}\gamma_L^{LW}} \quad \textbf{(2.62)}$$

Because $\gamma_L^{+}$and γ_L^{-} are zero and $\gamma_L^{LW}=\gamma_L$ so γ_S^{LW} can be determined. Contact angles gained from polar liquids provide γ_S^{+} and γ_S^{-} by solving a set of simultaneous Young's equations. When are known, the surface tension of the solid, γ_S, can be calculated from;

$$\gamma_S=\gamma_S^{LW}+2(\sqrt{\gamma_S^{-}\gamma_S^{+}}) \quad \textbf{(2.63)}$$

Furthermore, solid-liquid interfacial energy can be determined by the following formula;

$$\gamma_{SL}=\gamma_S+\gamma_L-2(\sqrt{\gamma_S^{LW}\gamma_L^{LW}}+\sqrt{\gamma_S^{-}\gamma_L^{+}}+\sqrt{\gamma_S^{+}\gamma_L^{-}}) \quad \textbf{(2.64)}$$

3. EXPERIMENTAL

In this part of the thesis, the experiments conducted for the determination of the contact angles of various rocks samples will be explained. The solid and liquid samples, the preparations of samples for the experiments, the equipment used in the experiments and the procedure of the experiments will be explained.

3.1 Materials

3.1.1 Solid Samples

In this study, samples of quartz, calcite, glass, Berea and Bentheim sandstones and carbonate rocks are used. Quartz (SiO_2, Silicon dioxide) and calcite ($CaCO_3$, Calcium carbonate) are the most common minerals in the face of the earth. Quartz and calcite are pure and single minerals whereas; sandstone and carbonate rocks contain many different constituents. However, sandstone is composed predominantly of quartz and carbonate rock is composed primarily of calcite mineral. Sandstone may also contain detritic feldspar and zircon, grona, topaz, colombite, tantalite, andalucite, magnetite, ilmenite, rutile, monazite, casiterite, gold and platinum. Calcite and carbonate rocks are the sedimentary rocks formed by chemical precipitation; moreover calcite is the most stable carbonate mineral (Kumbasar & Aykol, 1993).

Sandstones, having porosity value of about 21% and 23% respectively, are from Berea and Bentheim formations. Both sandstones and carbonate rocks are used for core analysis in Petroleum and Natural Gas Engineering Department's laboratories in ITU. Pure quartz and calcite samples are provided from the Department of Mining Engineering. In addition to this, soda-lime glass was used in the experiment to see if its wettability behavior was similar to that of quartz mineral. For thin layer wicking experiments, samples had to be crushed and then ground to powder size below 38 μm. Average sizes (d_{50}) and size distribution of powder particles were analyzed with Fritsch

Analysette 22 Compact Particle Size Analyzer that uses laser light scattering method for analyzing.

3.1.2 Liquids

In this study, distilled water, brine, kerosene, mineral oil and crude oil are used as the test liquids and heptane, octane, decane and dodecane are used as the standard liquids. Distilled water and %2 NaCl solution are used as water phase. Distilled water is produced by the help of the water purification system. Brine is prepared with weight/volume proportion method (Ucko, 1982). In this method, solution is prepared according to the total volume. The amount of solid in the solution can be found using the formula given below:

$$w/v = \frac{\text{amount of solid}}{(100 \text{ ml solution})(\text{volume of the solvent})} \quad \textbf{(3.1)}$$

Thus, 2 gr of NaCl is mixed with 100 ml distilled water in order to get 2% NaCl solution. Physical properties of distilled water and prepared brine are given in Table 3.1.

Table 3.1 : Physical Properties of Distilled Water and 2%NaCl Solution

Aqueous Phase	ρ, g/ cm^3 at 20°C	μ, cp at 20°C	γ, dyne/cm at 21°C
Distilled Water	1	1.0136	72.3
%2 NaCl	1.0241	1.0701	72.6

Kerosene, mineral oil and crude oil are used as oil phase. Refined kerosene has been provided from İzmit Tüpraş Refinery. A highly refined colorless white mineral oil is from Millers Oils Ltd. Brighouse, England and crude oil is supplied from Ozan Sungurlu field. The properties of refined oils and crude oil used in the wicking experiments are given in the Table 3.2.

Table 3.2 : The Properties of Oil

Oil Phase	ρ, g/ cm^3 at 20°C	μ, cp at 20°C	χ, dyne/cm at 21°C
Kerosene	0.800	1.3528	25.43
Mineral Oil	0.860	22.31	33.91
Crude Oil	0.919	27.00	10.47

To find effective pore radius, nonpolar alkanes which do not react with rock minerals were used. Thin layer wicking experiments were first conducted with apolar liquids heptane, octane, decane, and dodecane. Then, in estimation of effective pore radius of powder bed dodecane was chosen as the standard liquid. In addition to this, for the calculation of surface free energy components contact angle measurements were also conducted using polar ethylene glycol and apolar 1-bromonaphthelene and distilled water. These apolar and polar liquids were from Merck Company and provided by Surface Chemistry Laboratory located at the Department of Mining Engineering in ITU. Properties of chemicals used in the experiments are given in Table 3.3. (Karagüzel, 2005) and values of surface tension components and the viscosities of the liquids are given in the Table 3.4 (van Oss, 1994; Asmatalu 2001). Each liquid was put in a glass container and stored in dark and cool place.

Table 3.3 : Properties of Chemicals Used in the Experiments (Karagüzel, 2005)

Chemical's Name	Formula	Molecular Weight (g/ml)	Purety, %	Producer
Sodium Chloride	NaCl	58.44	99	Merck
Heptane	C_7H_{16}	100.21	>99	Merck
Octane	C_8H_{18}	114.23	>99	Merck
Decane	$C_{10}H_{22}$	142.29	>99	Merck
Dodecane	$C_{12}H_{26}$	170.34	>99	Merck
Bromonapthalene	$C_{10}H_7Br$	207.08	>99	Merck
Ethylene Glycol	$HOCH_2CH_2OH$	62.07	>99	Merck

Table 3.4 : Values of Surface Tension Components (in mJ/m^2) and Viscosities (in poise) of The Liquids used in Wicking Experiments (Van Oss, 1994; Asmatalu 2001)

Liquids	γ_L	γ_L^{LW}	γ_L^{AB}	$\gamma_L^{\oplus}$	γ_L^{-}	μ
Heptane	20.3	20.30	0	0	0.0	0.00409
Octane	21.6	21.60	0	0	0.0	0.00542
Decane	23.8	23.80	0	0	0.0	0.00907
Dodecane	25.4	25.35	0	0	0.0	0.01493
Bromonapthalene	44.4	44.40	0	0	0.0	0.04890
Etylene Glycol	48.0	29.00	19	1.92	47.0	0.19900
Water	72.8	21.80	51	25.5	25.5	0.01000

3.2. Pre-studies

3.2.1 Preparation of Powdered Samples

For thin layer wicking experiments, all solid samples had to be crushed to the size of sand particles and then ground to the size of powder. Samples were crushed with a hand-held hammer then sand-sized particles were ground using a mechanical agate mill. After that powdered samples were screened through a 38 μm mesh sieve. Over screen particles were ground until all material was below 38 μm.

3.2.2 Surface Tension Measurements

Surface tension measurements were achieved with the KSV Sigma 701 Tensiometer (Figure 3.1), which is a modular high performance PC controlled piece of equipment. It measures force on a sample being pulled through a fluid/fluid interface so surface or interfacial tension can be measured. There are two parts to the tensiometer. The measuring unit consists of a plastic lifting stage and a balance connected to a small wire hook for hanging samples. The tensiometer is controlled via a computer running windows operating system.

Figure 3.1: KSV Sigma 701 Tensiometer

In the experiments, a probe is hung on a balance and brought into a contact with the liquid interface tested. The forces experienced by the balance as the probe interacts with the surface of the liquid can be used to calculate surface tension. Two types of probes are commonly used, du Nouy Ring and the Wilhelmy Plate. In this study, du Nouy ring method was employed. It had been preferred for comparison purposes because many literatures have been obtained with the ring method. Furthermore, the wetted length of the ring exceeds that of the plate by a factor of 3. This leads a higher force on the balance and accordingly to a better accuracy. The figure of the du Nouy ring is given Figure 3.2.

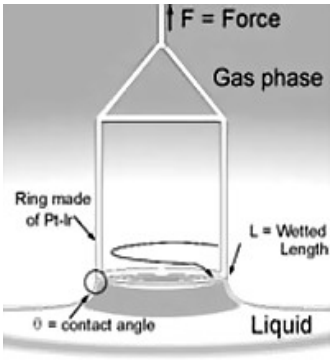

Figure 3.2 : Du Nouy Ring and its Interaction With The Liquid

The du nouy ring method utilizes the interaction of ring with the surface being tested. The ring was submerged below the interface and subsequently raised upwards. As the ring is moved upwards it raises a meniscus of the liquid. Eventually, the meniscus is torn from the ring and returned to its original position. The volume and thus the force exerted of the meniscus passes through a maximum value and begin to diminish prior to the actual tearing event. The process is shown in Figure 3.3. The calculation of the surface tension by this technique is based on the measurement of this maximum force.

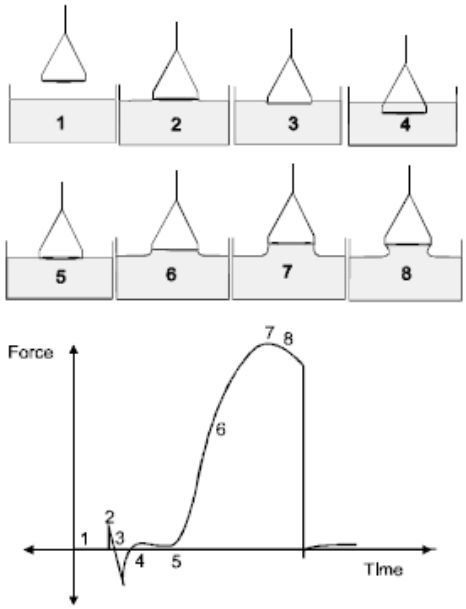

Figure 3.3 : Surface Tension Measurement Process With Du Nouy Ring Method

When the surface investigated was the interface of two immiscible liquids, interfacial tension measurements were conducted. This time, the denser liquid was poured into the sample vessel before the lighter liquid. Du Nouy ring was immersed into the lighter fluid until the ring was a few mm above the interface between the two immiscible liquids. Then measurements started and the ring submerged into the denser liquid and then rose through the lighter liquid. This action helped to measurement of interfacial tension.

3.2.3 Liquid Viscosity Measurements

Cannon Fenske Routine type viscometers (Figure 3.4) for transparent liquids were used for viscosity measurements. The Cannon glass viscometers let one to determine

viscosities using ASTM testing methods. The viscosity instruments were chosen according to the recommended viscosity ranges. The viscosity ranges are given in Table 3.5. According to this table, the viscosities of distilled water, kerosene, dodecane, and 2% NaCl solution were measured with size 50 and mineral oil was measured with size 100.

Table 3. 5 : The Viscosity Ranges of Cannon Fenske Viscometers

Size	Approx. viscometer constant, cSt/s	Range centistokes
25	0.002	0.5 to 2
50	0.004	0.8 to 4
75	0.008	1.6 to 8
100	0.015	3 to 15
150	0.035	7 to 35
200	0.1	20 to 100

Prior to the experiments, all glass parts were washed and rinsed with distilled water. Then, they were filled with chromic acid and allowed to stand for 2 days to remove any organic deposits or contaminations. After that they were washed with distilled water and then put into the oven to dry. Experiments were carried at in a constant temperature bath to measure viscosities of each liquid sample at different temperatures. The instrument was filled with the sample and put into the water bath. All the measurements were conducted after equilibrium time of approximately 15 minutes.

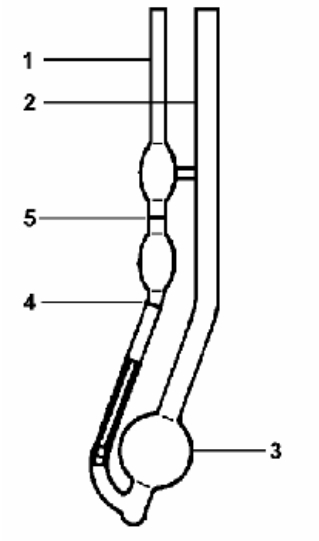

Figure 3.4 : Cannon Fenske Viscometer

In order to calculate kinematic viscosity in mm^2/s (cSt), efflux time in seconds was multiplied by the viscometer constant. The constant values at 40^oC and 100^oC were given, thus constants at other temperatures were obtained by interpolation. The viscosity in mPa.s (cP) can be obtained by the multiplication of the kinematic viscosity with the density in grams per milliliter.

3.3 Equipment

The main equipments used in the thin layer wicking experiments and contact angle measurements on flat surface will be given in this section. These are glass slides, wicking apparatus, stopwatch and goniometer.

3.3.1 Glass Slides

Wicking procedure was applied to the powdered sample layer spread over a glass slide. ISO Lab cut edged microscope slides, manufactured from high-optical grade soda-lime glass, were used in the experiments. The glass slides were chosen because glass has high surface energy and this will not impede the liquid adsorption into the powder (Chen, 1999). Slides were 26×76 mm in size and had 25.4 mm thickness. In each experiment approximately 35 slides were utilized with each powdered sample. On the one face of the glass slide, a scale with increments of 5 mm was marked for the observation of wetting front penetration. The cleanness of the slides was very important because any contamination on the glass surface could alter the adhesion of a powder layer and affect capillary rise. For this reason, each slide was thoroughly washed with detergent and rinsed with distilled water before coating process. Then they were kept in an oven 110^oC to achieve dry coated surfaces.

3.3.2 Wicking Apparatus

Coated glass slides were lowered into the beaker filled with wetting liquid by the wicking apparatus. The glass beakers used in the wicking experiments were thoroughly cleaned to avoid any contamination of wetting liquid. The wicking apparatus consists of adjustable stand, rotating handle, and fastener to which a coating sample is attached. Adjustable stand was controlled by the handle which is needed to lower and pull the

sample back (Tacibayev, 2004). The apparatus is described in Figure 3.5. Numbers represent; rotating handle (1), adjustable stand (2), hook (3) , fastener(4) , glass slide(5), glass container (6), wetting liquid (7), respectively.

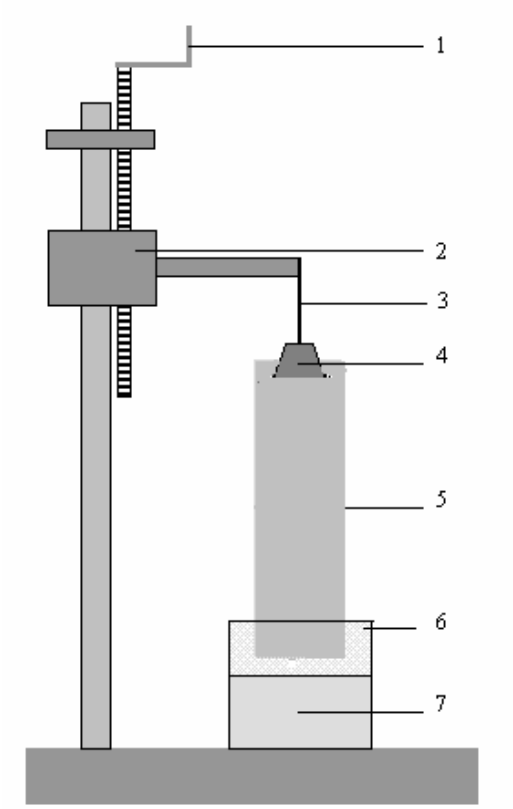

Figure 3.5 : Schematic Wicking Apparatus (Tajibaev, 2004)

3.3.3 Stopwatch

Digital stopwatch was used to detect the speed of propagation of the wetting front by recording the time needed for a liquid to travel a length of each increment on the scale. Time was recorded when the wetting front reached to the first 5 mm line till the 5^{th} line was wetted by the liquid. The t = 0 value is unknown because of the uncertainty of the time, when the liquid begins to wick through the powder film, but this is not a problem because the ratio is desired value which is the slope of the straight line and independent of the t = 0 value (Giese and van Oss, 2002).

3.3.4 Goniometer

It is an image based instrument that makes axisymmetrical drop shape analysis (ADSA) of liquid droplets on a flat surface. It is used to measure contact angle of a test liquid placed on a flat solid surface by using the sessile drop technique. The basic elements of a goniometer include a light source, sample stage, lens, and image capture. Contact angle can be evaluated directly by measuring the angle formed between the solid and the tangent to the drop surface. The Figure 3.6 shows the basic elements of a goniometer.

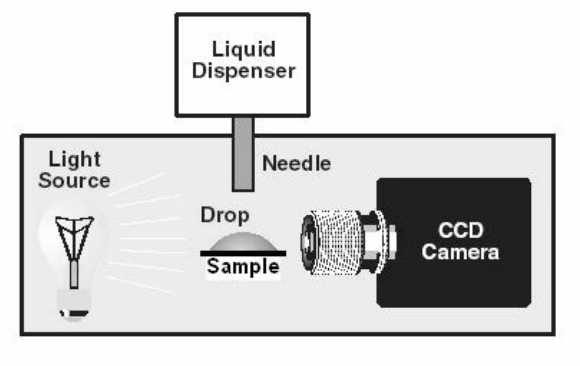

Figure 3.6 : Basic Elements of a Goniometer

3.4 Procedure

3.4.1 Contact Angle Measurements on Powdered Surface

The thin layer wicking method was used in order to determine the contact angles of the powdered samples. This technique covers the deposition of powdered sample on the glass slides and determination of the contact angles of the powder using the Washburn equation.

3.4.1.1 Preparation of the coated sample

Aqueous suspension of fine mineral particles was transferred on to clean glass microscope slides with a pipette and then water was evaporated leaving uniform thin layer of mineral powder. The concentration of powder in the water which gave the desired thickness and uniformity of film was investigated and decided to use 4% solids ratio suspensions. However, according to Holysz (1998), the measured contact angle values are independent from the thickness of the layer. He has studied different

thickness of layers and proved that even up to 2 mm thick, good liquid penetration values were obtained. This is important because thin layer were prepared from the deposited layer of less controlled thicknesses.

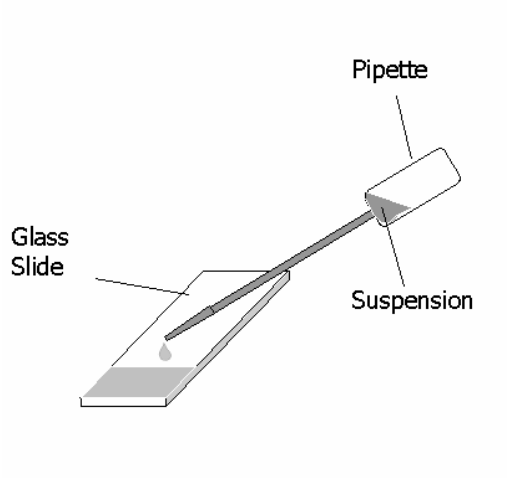

Figure 3.7 : Preparation of Coated Slides (Tajibaev, 2004)

To prepare the coated slides for wicking, the following procedure was applied illustrated in Figure 3.7. Four grams of sample was dispersed in 100 ml of distilled water and agitated by a magnetic stirrer to keep the particles in suspension. During stirring, aliquots of 3 ml were withdrawn with a pipette and spread equally over clean glass slide. In order to get uniform layer of coating, the suspension was accurately dispersed drop by drop on the glass surface from one end to another until the whole surface was covered with suspension. After water was evaporated at the room temperature for 24 hours, the coated slides were dried in an oven at 110^{o}C for 1 hour to remove any residual water remaining within pores. The residual water can dilute the wicking liquids and change their surface tensions and viscosities; this may cause a change in of the capillary rise pattern (Karagüzel et al., 2005). This procedure was applied to obtain, a uniform thin layer of powdered sample adhering to the surface of the glass.

3.4.1.2 Wicking experiment

Wicking experiments were performed by immersing the slides vertically into 5 mm depth of wicking liquids in a beaker. Prior to immersion tests, the glass slide was kept inside a closed container for about 1 hour, to allow the powder to come in to contact with the vapor of the wicking liquid for equalizing the spreading pressure (Yıldırım,

2001). Once the equilibrium was attained, the slide was immersed into the liquid and at this instant; the stopwatch was started to measure the time at which the liquid front reaches each of the marks on the slide. The rise of the liquid up to 2 cm from the liquid entry level was observed. About 35 slides were prepared for each sample and each measurement was repeated at least 3 times. The average wicking times for each sample were given in Appendix A. The schematic description of thin layer wicking experiment is given in Figure 3.8.

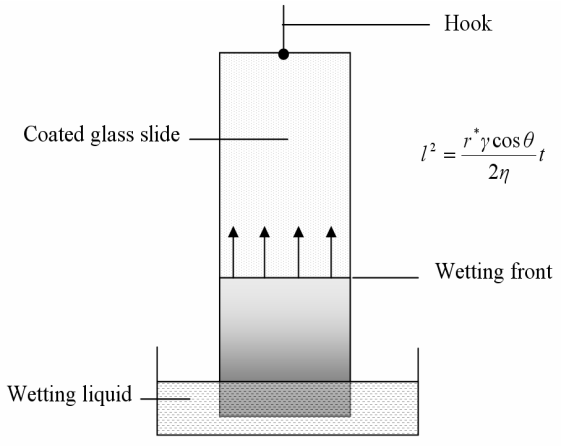

Figure 3.8 : Schematic Representation of Thin Layer Wicking Experiment (Tajibaev,2004)

3.4.1.3 Determination of effective pore radius

The value of r^* in Washburn equation which is the pore size characteristics of a powder bed was determined using completely wetting liquids (non-polar) having low energy. In Wu and Nancollas's paper (1999), it was stated that using spreading liquids like n-alkanes, θ remains exactly equal to zero in Washburn equation, so that $cos\theta$ =1, as a result of the formation of precursor film. By the elimination of contact angle value, effective pore radius can be obtained.

Experiments were conducted with heptane, octane, decane and dodecane owing to their low surface tension and non-polarity. It was observed that experiments conducted with heptane and octane gave smaller value of r^*. Holysz (1998) explained the reason for the smaller r^* value with the partially evaporation of these hydrocarbons from the surface during the penetration process. Taking r^* constant, a liquid that yielded the highest value

of $r^*cos\theta$ was considered to be a standard liquid. In this case, also taking into account volatility and viscosity best results were obtained with dodecane. Therefore, dodecane was chosen as the standard liquid to be used in wicking experiment to find r^*.

3.4.1.4 Contact angle measurement

During the wicking experiment conducted with the standard liquid, the travel distance (l^2) was recorded as a function of time (t). The plot of l^2 versus t formed a straight line. Because the standard liquid completely wets the surface, $\cos\theta$ equals to 1. So r^*, which is the radius of a capillary tube that would wick a given liquid at the same rate as the powder would, can be easily calculated. After the mean pore radii determination, the same wetting tests were performed with test liquid. In these tests, again linear plots of l^2 versus t were determined. Therefore, the contact angle values of test liquids were calculated from the slopes and obtained r^* values by the help of the Washburn equation.

3.4.2 Contact Angle Measurements on Flat Surface

Contact angles of polished solid samples may be measured using sessile drop method. This time, the experiments conducted on flat solid surface and the results of thin layer wicking method are compared with goniometric measurements.

3.4.2.1 Goniometric measurements

The contact angle measurements were conducted on polished surfaces of quartz, calcite and glass slide employing sessile drop technique. In this method, a small drop of liquid was placed on the surface of a polished sample with a syringe and the contact angle was measured using a goniometer. The static angle formed between the liquid drop and flat solid surface was read from the scale of the goniometer with the help of a microscope. These experiments were performed for distilled water, brine, kerosene, dodecane and mineral oil on glass slide, polished quartz and calcite mineral surfaces. The measured values are given in Table 3.6. These results were compared with contact angle values obtained from thin layer wicking method.

Table 3.6 : Results of Goniometric Measurements

Liquids	θ^o, on Glass Slide	θ^o, on Polished Quartz	θ^o, on Polished Calcite
Distilled Water	10	30	75
Brine	10	35	70
Dodecane	0	0	16
Kerosene	0	0	10
Mineral Oil	0	0	12

3.4.3 Determination of the Surface Energy Components

Oss-Chaudary-Good equation characterizes a solid surface in terms of its surface free energy components. The values of $\gamma^{LW}, \gamma_L^{\oplus}$ and γ_S^{-} for a solid can be derived from the contact angle values obtained by the thin layer wicking method, provided that the surface tension properties of the liquid are known. To determine these values, three wicking tests were conducted with polar water and ethylene glycol and apolar bromonapthalene using the same experimental procedure. $\gamma_L^{\oplus}$ and γ_S^{-} values of bromonapthalene are zero so γ_S^{LW} was easily determined from the contact angle measurement. As γ_S^{LW} was estimated, the values of $\gamma_L^{\oplus}$ and γ_S^{-} were determined from the contact angle measurements conducted with water and ethylene glycol. Water has the largest value of the Lewis acid parameter. Since the $\gamma_L^{\oplus}$ interacts with the γ_S^{-}, a large $\gamma_L^{\oplus}$ value ensures that the product of $\gamma_L^{\oplus}\gamma_S^{-}$ will be large yielding a well determined value of γ_S^{-}. Other polar liquids have low and similar $\gamma_L^{\oplus}$ values that create difficulties in finding a unique and reliable value of γ_S^{-}. Therefore, water must be one of the liquids in energy calculations (Giese and van Oss, 2002). Once the three surface tensions are obtained, the surface tension of the solid, $\gamma_{s,}$ can be determined. It should be pointed out that by test liquids, it is not possible to determine the whole surface free energy of a substance but only to estimate certain components of the surface free energy, usually those which are present in the test liquids (Karagüzel et al. 2005). The thin layer wicking experiments were also performed to determine the surface energy components of calcite and glass samples with polar distilled water and ethylene glycol and apolar bromonapthalene. By the help of their $\cos\theta$ values and known parameters of liquids, the surface free energy components were calculated and tabulated in Table 3.

Table 3.7 : The Surface Free Energy Components of Calcite and Glass

Samples	γ_S	γ_S^{LW}	γ_S^{AB}	$\gamma_S^{\oplus}$	γ_S^{-}	γ_{SL}
Calcite	36.61	29.17	7.44	0.68	20.36	4.57
Glass	49.54	21.48	28.06	7.08	27.80	-1.56

3.5 The Procedure for Calculations

3.5.1 Contact Angle Calculations

The composition of Berea sandstone that was used in sample calculations is given Table3.8.

Table 3.8 : Composition of Berea Sandstone (Ma & Morrow, 1991)

Mineral	%
Quartz	78.5
Rock fragments	8.6
Dolomite	2.5
Calcium oxide	0
Untwinned feldspar	5.3
Microline feldspar	0.7
Chert	1.6
Kaolinite	2.8
Total solids	100
Porosity (%)	18.3

3.5.1.1 Vapor-liquid-solid interface

For the calculation of contact angle formed between air-water-solid surface two wicking experiments were done. To determine effective radius, wicking experiments were conducted by dodecane with at least on three coated slides. Test results are shown in Table 3.9.

Table 3.9 : Distance against Wicking Time For Dodecane

		Wicking Time, seconds		
Distance, l, cm	l^2, cm^2	t_1, s	t_2, s	t_3, s
0.5	0.25	7	6	10
1	1	36	34	38
1.5	2.25	75	74	84
2	4	135	127	157

The given data was plotted on the graph in order to obtain the slopes of (l^2/t) for dodecane and to calculate *r** in Figure 3.9.

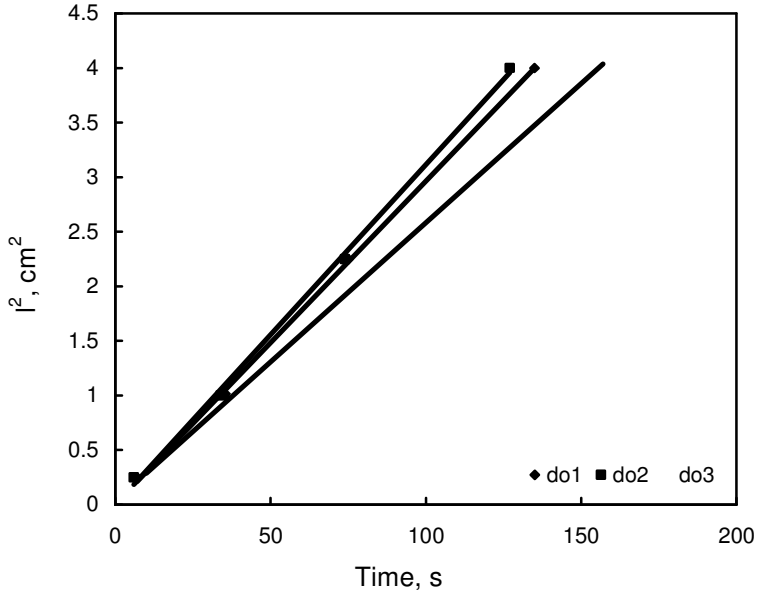

Figure 3.9 : Wicking Experiment of Berea Sample with Dodecane

The average slope value for dodecane was found as 0.02876. $\left(l^2/t\right)_d =$. Equation (2.39), was used for the calculations of effective pore radius. In calculations, $\gamma_L = 25.38$ dyne/cm and $\mu = 0.015454$ Poise (at 20°C) for dodecane were used.

$$r^* = \frac{2\mu}{\gamma}\frac{l^2}{t} = \frac{2\times 0.015454}{25.38}0.02876 = 3.503\times 10^{-5}(\text{cm})$$

To determine contact angle of water the wicking experiments were conducted using water making at least three repetitions, and the results are given in Table 3.10.

Table 3.10 : Distance against Wicking Experiment Time for Water

		Wicking Time, seconds		
Distance, l, cm	l^2, cm^2	t_1, s	t_2, s	t_3, s
0.5	0.25	8	7	6
1	1	17	17	20
1.5	2.25	36	34	36
2	4	55	54	60

The given data were plotted on the graph in order to obtain the slopes of l^2/t for water. The average slope of the graph (Fig.3.10) plotted by these data was found as $\left(l^2/t\right)_w = 0.0795$.

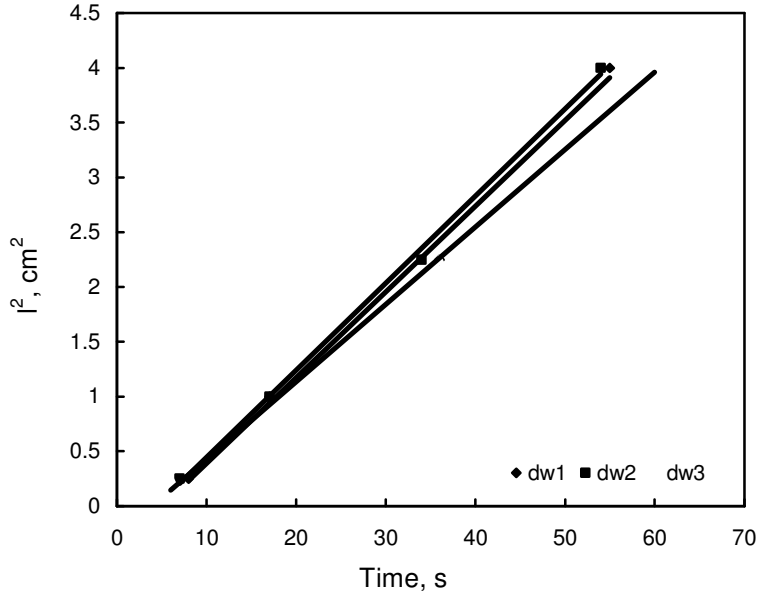

Figure 3.10 : Wicking Experiment of Berea Sample with Water

The contact angle of distilled water was calculated using Equation (2.40). In these equations, the values of $\gamma_L = 72.3$ dyne/cm and $\mu = 0.010136$ Poise (at 20^oC) for distilled water were used.

$$cos\theta = \frac{2\mu}{r^*\gamma}\frac{l^2}{t} = \frac{2\times 0.010136}{3.503\times 10^{-5}\times 72.3}0.0795 = 0.636$$

$$\theta = cos^{-1}\left(\frac{2\eta}{r^*\gamma}\frac{l^2}{t}\right) = cos^{-1}\left(0.636\right) = 51$$

Thus, the value of the contact angle of distilled water with respect to the particles' surface for the Berea sandstone sample was determined as 51^o.

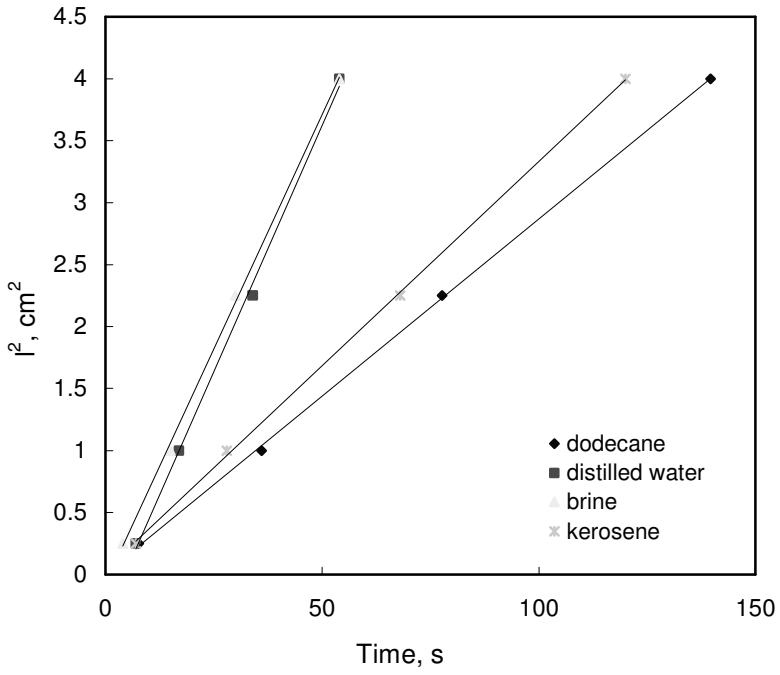

Figure 3.11 : The Results of Wicking Experiments for Dodecane, Distilled Water, Brine and Kerosene on Berea Sample

Contact angles of 2% NaCl solution, kerosene, mineral oil and crude oil on this sample were calculated in the same manner. The slopes of these liquids are given in Figure 3.11 and Figure 3.12. According to these results, the calculated contact angle values are given in Table 3.11.

Table 3.11 : The Calculated Contact Angle Values of Test Liquids on Berea Sample

	θ^{o}
Distilled Water	51
2% NaCl solution	50
Kerosene	25
Mineral Oil	45
Crude Oil	70

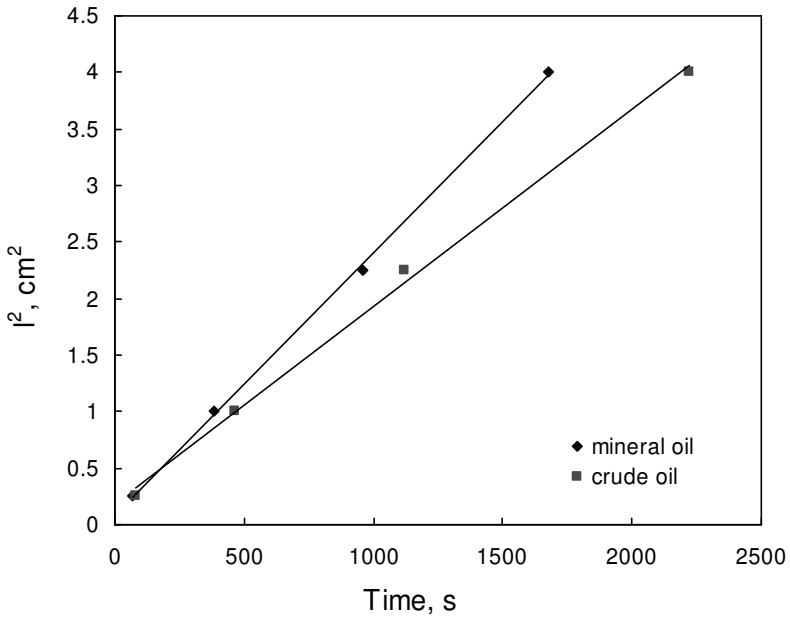

Figure 3.12 : The Results of Wicking Experiments for Mineral Oil and Crude Oil on Berea

3.5.1.2 Liquid-liquid-solid interface

To estimate the contact angle formed on the distilled water-kerosene-solid interface, Equation (2.9) was used. Contact angles of distilled water θ_{dw} and kerosene θ_k on Berea sandstone powdered samples were calculated as 51° and 25°, respectively. The interfacial tension between distilled water and kerosene $\gamma_{dw\text{-}k}$ is 43.5 dyne/cm. Surface tensions of distilled water, γ_{dw}, and kerosene, γ_k, are 72.3 dyne/cm and 25.43 dyne/cm, respectively.

$$cos\theta_{dw\text{-}k} = \frac{\gamma_{dw} cos\theta_{dw} - \gamma_k cos\theta_k}{\gamma_{dw\text{-}k}} = \frac{72.3 \times \cos(51) - 25.43 \times \cos(25)}{43.5} = 0.5278 \qquad \textbf{(2.9)}$$

$$\theta_{dw\text{-}k} = cos^{-1}(52.78) = 58$$

Thus, the contact angle value of distilled water/ kerosene/ Berea sandstone sample was determined as 58^{o}.

3.5.1.3 Alternative determination of the *r** and its effect on contact angle measurements

In this part, the thin layer wicking experiments are performed with heptane, octane, decane and dodecane. The test results are given in Table 3.12 and the effective pore radius is determined as r*= 0.0008 from the slope of γ_L-$2\mu l^2/t$ graph in Figure 3.13.

Table 3.12 : Thin Layer Wicking Results for Apolar Liquids

Liquids	γ (dyne/cm)	$2^*\mu^*l^2$ / t
Heptane	20.3	0.00060
Octane	21.6	0.00071
Decane	23.8	0.00076
Dodecane	25.38	0.00103

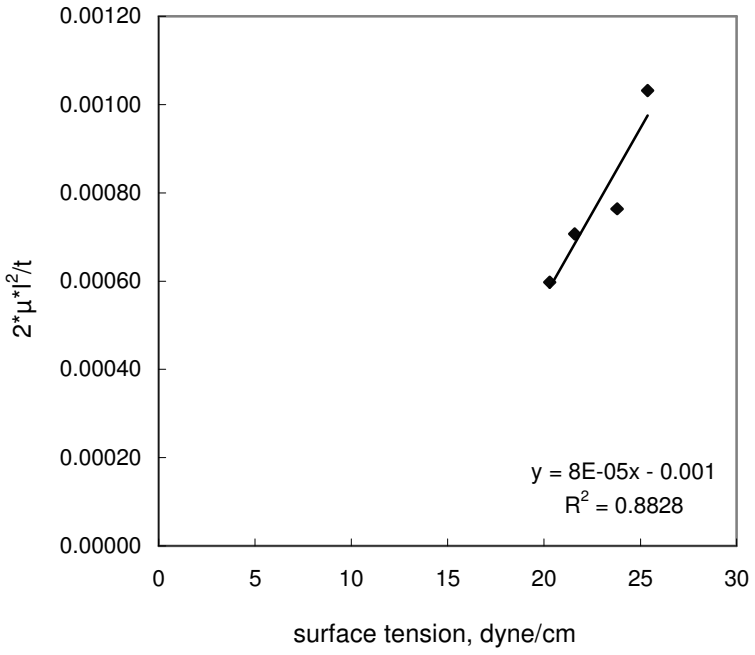

Figure 3.13 : Determination of Effective Pore Radius from Apolar Liquids

The contact angles of the Berea sandstone are calculated with the Washburn equation by using the slope $r^* = 0.00008$ in Figure 3.13. The calculated contact angle values and are given in Table 3.13. When these results are compared with the results determined from using only dodecane as the standard liquid presented in Table 3.12 and 3.13, it can be observed that dodecane is found to be the most suitable alkane to be used as a standard liquid for effective pore radius measurements in Thin Layer Wicking experiments.

Table 3.13 : The Contact Angle Values With respect to Apolar Liquids and Dodecane

	With Apolar Liquids	With Only Dodecane
	θ^o	θ^o
Distilled Water	72	51
Brine	75	50
Kerosene	65	25
Mineral Oil	70	45
Crude Oil	80	70

3.5.2 Surface Free Energy Calculations

Solid surface free energy can be calculated from the summation of the Lifshitz van der Walls and acid-base interactions from the liquids that have known surface tensions. Here, the powdered calcite sample's free surface energy is calculated from the contact angles of water, bromonapthelene and ethylene glycol found with the thin layer wicking experiments.

The Thin Layer Wicking measurements for bromanapthalene and ethylene glycol are shown in the Figure 3.14. By using these l^2/t values in Washburn equation, the $\cos\theta$ values of bromonapthalene and ethylene glycol are found 0.621 and 0.668, respectively. Also the $\cos\theta$ of distilled water is found 0.423. The necessary values of liquids that are used in these calculations are given in Table 3.14.

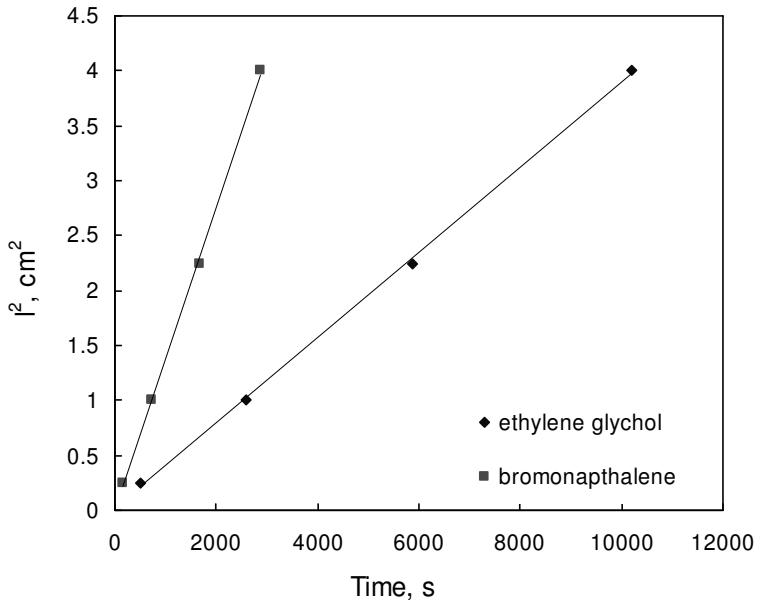

Figure 3.14 : Thin Layer Wicking Experiment for Bromonapthalene and Ethylene Glycol on Calcite Sample

Table 3.14 : The Surface Tensions and $\cos\theta$ Values of Liquids on Calcite

Liquids	γ_L	γ_L^{LW}	γ_L^{AB}	$\gamma_L^{\oplus}$	γ_L^{-}	**Cos θ**
Bromonapthalene	44.4	44.40	0	0	0.0	0.621
Ethylene Glycol	48.0	29.00	19	1.92	47.0	0.668
Distilled Water	72.8	21.80	51	25.5	25.5	0.423

For the calculation of the Lifshitz van der Walls energy bromanapthalene is used because it has no acid-base interaction. For this reason Oss-Chaudary-Good equation (Eq.2.61) becomes Equation 2.61 ;

$$(1+\cos\theta)\gamma_L = 2(\sqrt{\gamma_S^{LW}\gamma_L^{LW}})$$

$$(1+0.621)\gamma_L = 2(\sqrt{\gamma_S^{LW}44.4})$$

$$\gamma_S^{LW} = 29.17\,mJ/m^2$$

After that, solid surface's energy components and solid surface free energy can be calculated from the polar liquids; distilled water and ethylene glycol using again the OCG equation (Eq.2.61). The calculations for distilled water are given below:

$$(1+\cos\theta)\gamma_L = 2(\sqrt{\gamma_S^{LW}\gamma_L^{LW}} + \sqrt{\gamma_S^-\gamma_L^+} + \sqrt{\gamma_S^+\gamma_L^-})$$
$$(1+0.4234)72.3 = 2(\sqrt{29.17\times21.8} + \sqrt{\gamma_S^-25.5} + \sqrt{\gamma_S^+25.5})$$
$$26.23 = 5.05\sqrt{\gamma_S^-} + 5.05\sqrt{\gamma_S^+}$$

There appears an equation having two unknowns. Furthermore, same equation is used for ethylene glycol and another equation having two unknowns is obtained.

$$(1+\cos\theta)\gamma_L = 2(\sqrt{\gamma_S^{LW}\gamma_L^{LW}} + \sqrt{\gamma_S^-\gamma_L^+} + \sqrt{\gamma_S^+\gamma_L^-})$$
$$(1+0.668)48 = 2(\sqrt{29.17\times29} + \sqrt{\gamma_S^-1.92} + \sqrt{\gamma_S^+47})$$
$$10.95 = 1.39\sqrt{\gamma_S^-} + 6.86\sqrt{\gamma_S^+}$$

When we solve these two equations simultaneously we can find γ_S^- = 20.36 mJ/m^2 and γ_S^+ = 0.68 mJ/m^2. Acid-base interaction energy can be calculated with Equation (2.52).

$$\gamma_S^{AB} = 2\sqrt{\gamma_S^+\gamma_S^-}$$
$$\gamma_S^{AB} = 2\sqrt{20.36\times0.68}$$
$$\gamma_S^{AB} = 7.44\,\text{mJ/m}^2$$

Then calcite surface free energy is the summation of γ_S^{AB} and γ_S^{LW} (Eq. 2.63).

$$\gamma_S = \gamma_S^{LW} + \gamma_S^{AB} = 29.17 + 7.44 = 36.61\,\text{mJ/m}^2$$

Lastly, calcite-water interfacial energy can be determined by Equation (2.64) ;

$$\gamma_{SL} = \gamma_S + \gamma_L - 2(\sqrt{\gamma_S^{LW}\gamma_L^{LW}} + \sqrt{\gamma_S^-\gamma_L^+} + \sqrt{\gamma_S^+\gamma_L^-})$$
$$\gamma_{SL} = 36.61 + 72.3 - 2(\sqrt{29.17\times21.8} + \sqrt{20.36\times25.5} + \sqrt{0.68\times25.5})$$
$$\gamma_{SL} = 4.57\,\text{mJ/m}^2$$

4. EVALUATION OF EXPERIMENTAL RESULTS

In this section, the results of Thin Layer Wicking experiments conducted on quartz, glass, Berea and Bentheim sandstones, calcite and carbonate rocks using standard (dodecane) and test liquids (distilled water, brine, kerosene, mineral oil, and crude oil) will be evaluated. The comparison of apolar standard liquids (heptane, octane, decane, and dodecane) which were used to find average pore radius will be given. Furthermore, the surface free energy calculations for calcite and glass samples due to distilled water, obtained by the help of Thin Layer Wicking results conducted with polar bromanapthalene and apolar ethleyene glycol will be compared.

4.1 The Results of Thin Layer Wicking Experiments

4.1.1 The Results For Quartz

The results of Thin Layer Wicking Experiments with respect to dodecane and test liquids - distilled water, brine, kerosene, mineral oil - for quartz mineral are given in Figures 4.1 and 4.2. The result of mineral oil has to be given in another plot because of longer wicking time in comparison to the other liquids due to mineral oil's lower wicking tendency. It can be seen that distilled water and brine give similar wicking rate like dodecane and kerosene do.

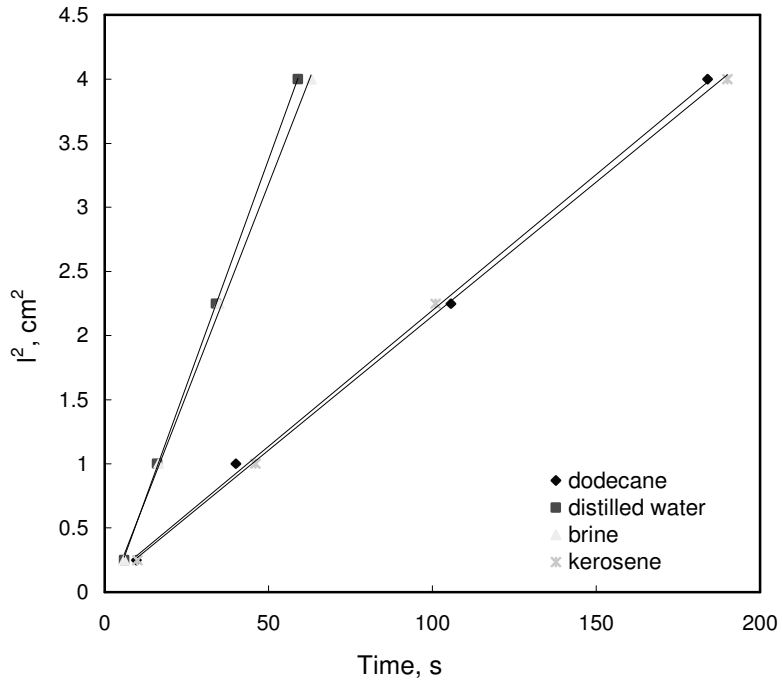

Figure 4.1 : The Results of Wicking Experiments for Dodecane, Distilled Water, Brine and Kerosene on Quartz

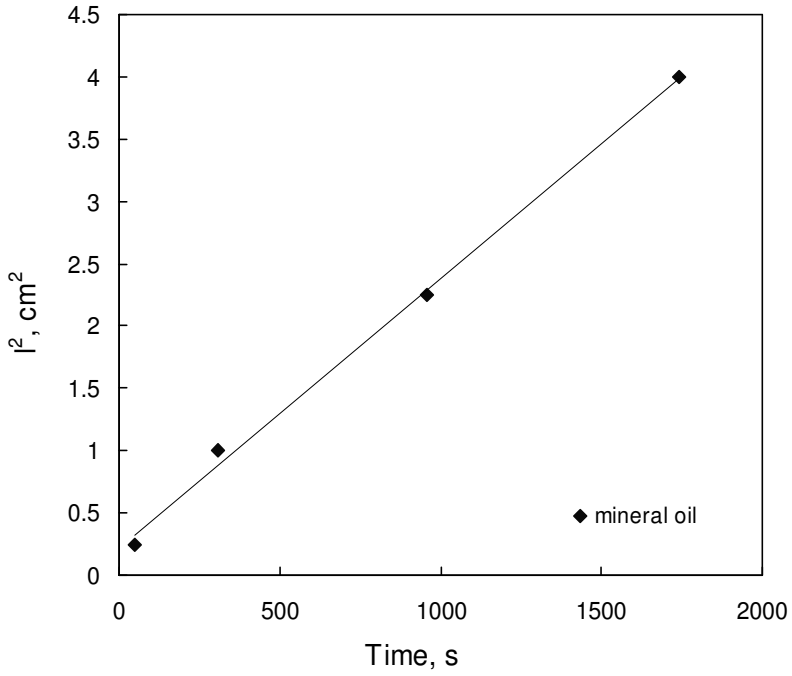

Figure 4.2 : The Results of Wicking Experiments for Mineral Oil on Quartz

The calculated contact angle values according to test liquid/air/quartz system are given in Table 4.1. Consistent with the results of goniometer, the distilled water and brine has low contact angle values but mineral oil has lower value showing higher spreading tendency. Kerosene shows complete spreading over quartz mineral. Besides, the calculated contact angle values according to liquid/liquid phase/quartz system are given in Table 4.2. From these results, it can be concluded that quartz mineral is strongly water wet according to the cut-off values cited in the literature (Morrow, 1991).

Table 4.1 : The Calculated Contact Angle Values of Test Liquids for Quartz

Liquids	θ^o
Distilled Water	26
Brine	26
Kerosene	0
Mineral Oil	15

Table 4.2 : The Calculated Contact Angle Values of Liquid-Liquid- Quartz

Liquids	θ^o
Distilled Water - Kerosene	24
Brine - Kerosene	13
Distilled Water- Mineral Oil	47
Brine - Mineral Oil	32

4.1.2 The Results For Glass

The results of Thin Layer Wicking Experiments conducted using dodecane and test liquids - distilled water, brine, kerosene - for glass are given in Figure 4.3 Also, the results for mineral oil is given in Figure 4.4. It can be seen that distilled water and brine give similar wetting tendencies.

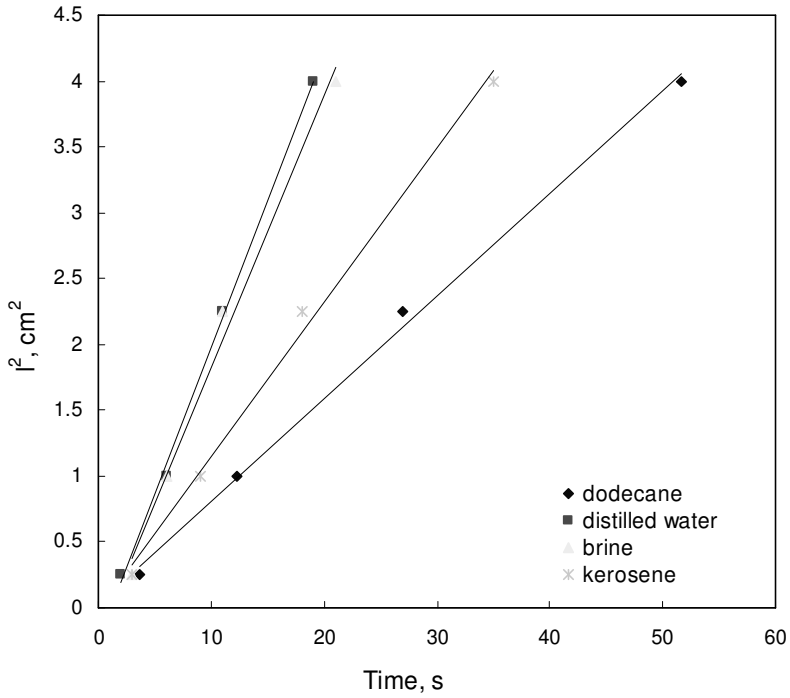

Figure 4.3 : The Results of Wicking Experiments for Dodecane, Distilled Water, Brine and Kerosene on Glass

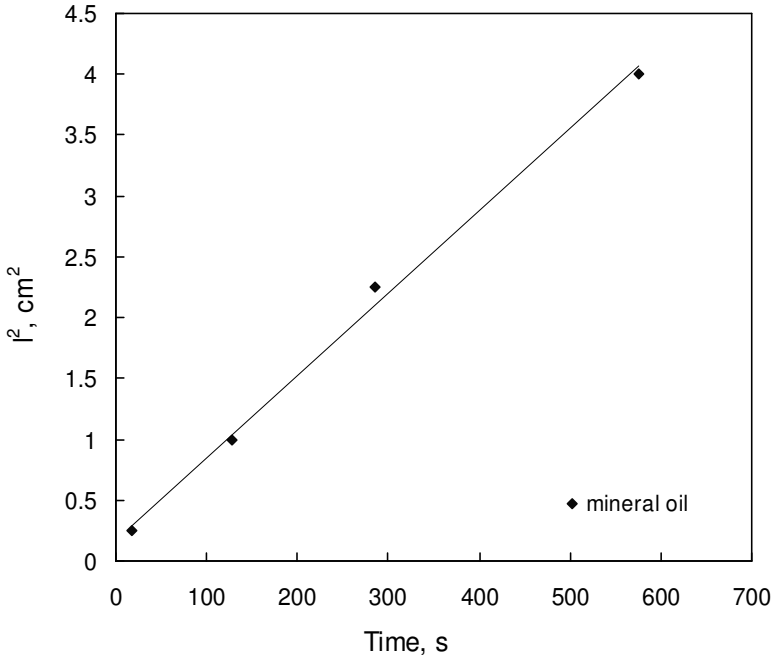

Figure 4.4 : The Results of Wicking Experiments for Mineral Oil on Glass

The calculated contact angle values according to test liquid/air/glass system are given in Table 4.3. Consistent with the results of goniometer, kerosene and mineral oil has lower value showing higher spreading tendency than the distilled water and brine. Besides, the calculated contact angle values according to liquid /liquid/ glass system are given in Table 4.4. From these results, it can be concluded that glass used in this study is water wet according to the cut-off values cited in the literature (Morrow, 1991).

Table 4.3 : The Calculated Contact Angle Values of Test Liquids for Glass

Liquids	θ^o
Distilled Water	45
Brine	48
Kerosene	6
Mineral Oil	5

Table 4.4 : The Calculated Contact Angle Values of Liquid-Liquid-Solid Interface for Glass

Liquids	θ^o
Distilled Water - Kerosene	53
Brine - Kerosene	56
Distilled Water- Mineral Oil	68
Brine - Mineral Oil	68

4.1.4 The Results For Berea Sandstone

The results of Thin Layer Wicking Experiments carried out with dodecane and test liquids - distilled water, brine, kerosene - for Berea sandstone are given in Figure 4.5 Furthermore; the results for mineral oil and crude oil are given in Figure 4.6. It can be seen that distilled water and brine give similar wetting tendencies. In addition mineral oil and crude oil have higher wicking properties.

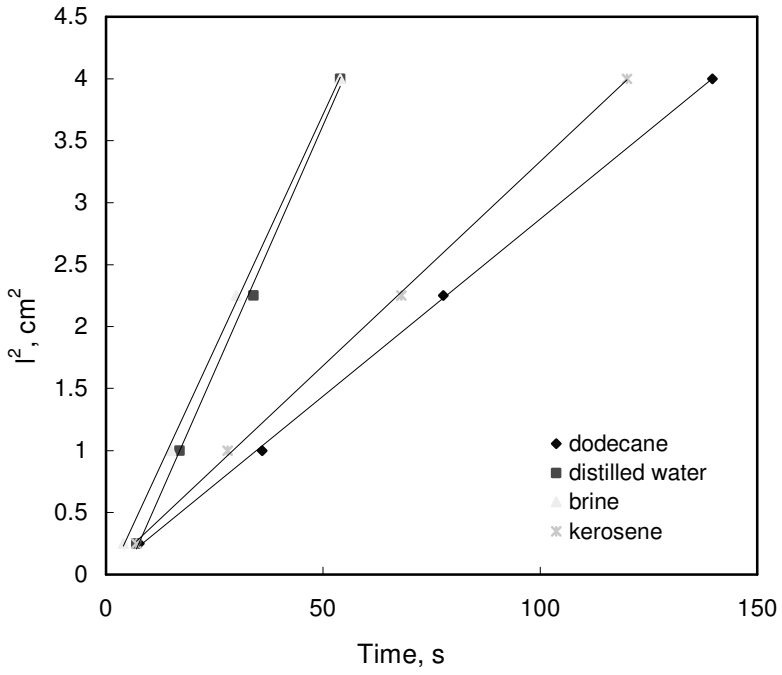

Figure 4.5 : The Results of Wicking Experiments for Dodecane, Distilled Water, Brine and Kerosene on Berea

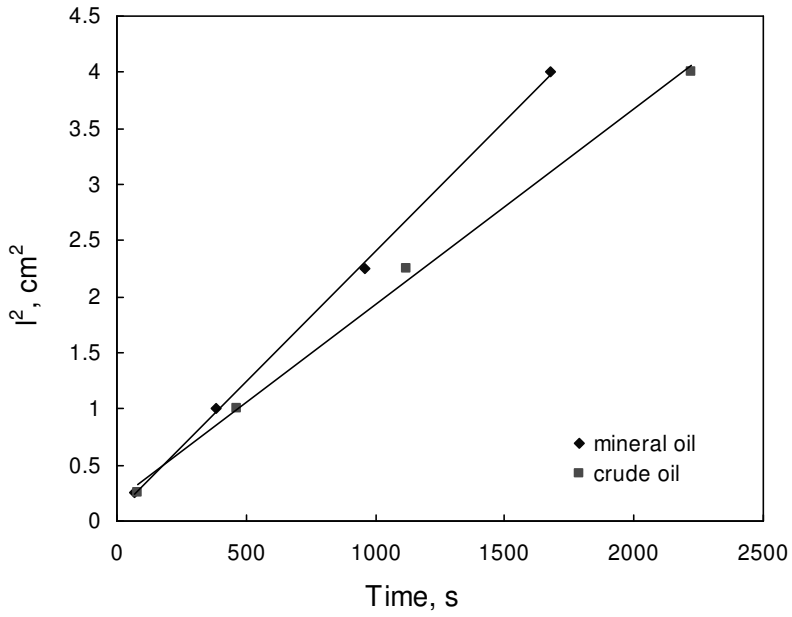

Figure 4.6 : The Results of Wicking Experiments for Mineral Oil and Crude Oil on Berea

The calculated contact angle values according to test liquid/ air / Berea system are given in Table 4.5. The thin layer wicking experiment was also performed for mineral oil and crude oil and it can be seen that crude oil gives the highest contact angle value. Besides, the calculated contact angle values according to liquid/ liquid/ Berea system are given in Table 4.6. From these results, it can be concluded that Berea sandstone used in this study is water wet according to the cut-off values cited in the literature (Morrow, 1991).

Table 4.5 : The Calculated Contact Angle Values of Test Liquids for Berea

Liquids	θ^o
Distilled Water	51
Brine	50
Kerosene	25
Mineral Oil	45
Crude Oil	70

Table 4.6 : The Calculated Contact Angle Values of Liquid-Liquid-Solid Interface for Berea

Liquids	θ^o
Distilled Water - Kerosene	58
Brine - Kerosene	55
Distilled Water- Mineral Oil	65
Brine - Mineral Oil	68

4.1.4 The Results For Bentheim Sandstone

The results of Thin Layer Wicking Experiments employing dodecane and test liquids - distilled water, brine, kerosene - for Bentheim sandstone are given in Figure 4.7 It can be seen that wicking behaviors of dodecane and kerosene differ from distilled water and brine. Also, the results for mineral oil is given in Figure 4.8.

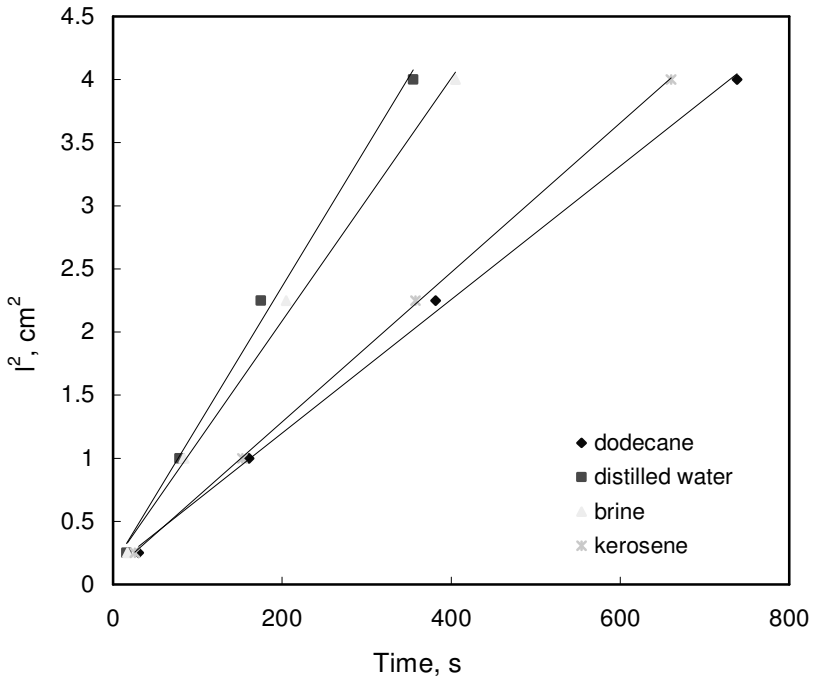

Figure 4.7 : The Results of Wicking Experiments for Dodecane, Distilled Water, Brine and Kerosene on Bentheim

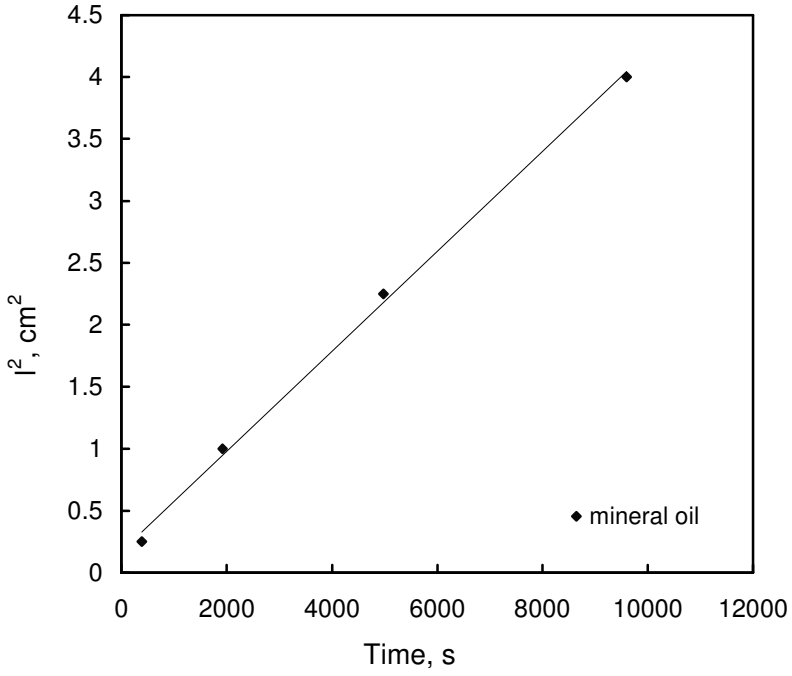

Figure 4.8 : The Results of Wicking Experiments for Mineral Oil on Bentheim

The calculated contact angle values for test liquid/air /Bentheim system are given in Table 4.7. Kerosene has lower contact angle value which represent higher wetting ability. Also mineral oil has lower contact angle values than aqueous phases. Furthermore, the calculated contact angle values in the case of aqueous phase/ oil phase/Bentheim system are given in Table 4.8. From these results, it can be concluded that Bentheim sandstone has intermediate wetting according to the cut-off values cited in the literature (Morrow, 1991).

Table 4.7 : The Calculated Contact Angle Values of Test Liquids for Bentheim

Liquids	θ^o
Distilled Water	62
Brine	64
Kerosene	9
Mineral Oil	34

Table 4.8 : The Calculated Contact Angle Values of Liquid-Liquid-Solid Interface for Bentheim

Liquids	θ^o
Distilled Water - Kerosene	79
Brine - Kerosene	81
Distilled Water- Mineral Oil	83
Brine - Mineral Oil	85

4.1.5 The Results For Calcite

The results of Thin Layer Wicking Experiments using dodecane and test liquids - distilled water, brine, kerosene - for calcite mineral are given in Figure 4.9, and the results for mineral oil and crude oil are given in Figure 4.10. It can be seen that distilled water and brine have similar wetting tendencies, while mineral oil and crude oil have higher wicking properties. Mineral oil and crude oil have longer wicking time due to their higher wicking properties.

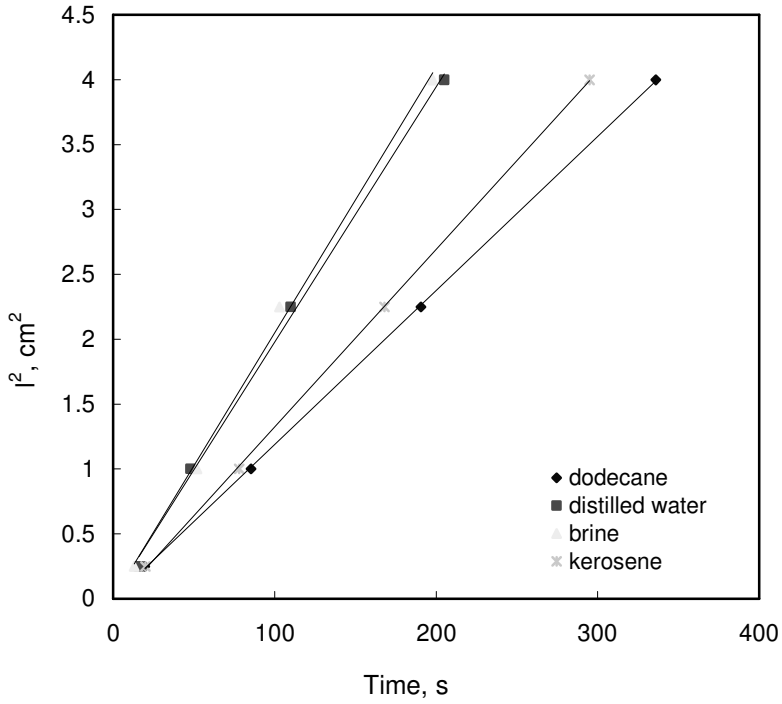

Figure 4.9 : The Results of Wicking Experiments for Dodecane, Distilled Water, Brine and Kerosene on Calcite

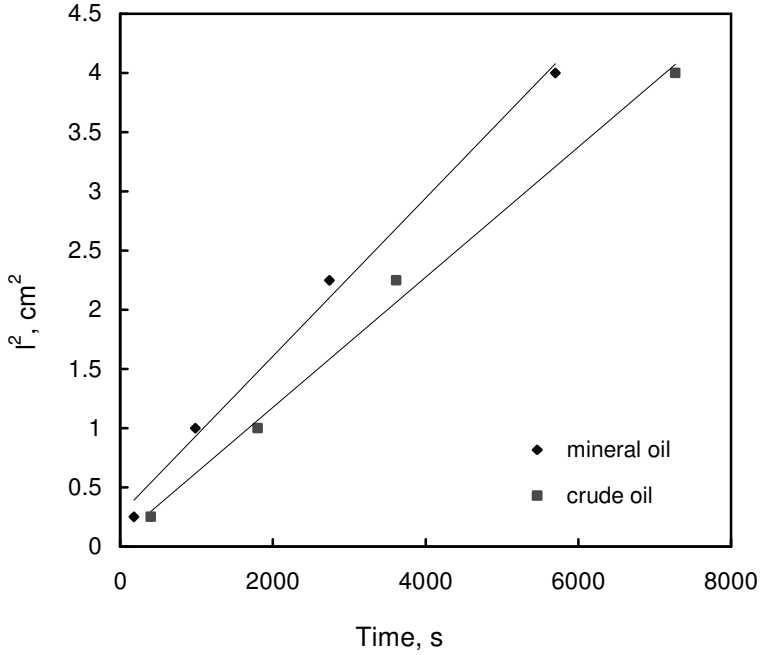

Figure 4.10 : The Results of Wicking Experiments for Mineral Oil and Crude Oil on Calcite

The calculated contact angle values according to test liquid/ air /calcite system are given in Table 4.9. Kerosene has zero contact angle value which represents complete wetting. Also mineral oil has lower contact angle values than aqueous phases. In addition, crude oil has the highest contact angle value. Furthermore, the calculated contact angle values for aqueous phase/ oil phase/ calcite system are given in Table 4.10. From these results, it can be concluded that calcite mineral used in this study has intermediate wetting according to the cut-off values cited in the literature (Morrow, 1991).

Table 4.9 : The Calculated Contact Angle Values of Test Liquids for Calcite

Liquids	θ^o
Distilled Water	67
Brine	65
Kerosene	0
Mineral Oil	32
Crude Oil	71

Table 4.10 : The Calculated Contact Angle Values of Liquid-Liquid-Solid Interface for Calcite

Liquids	θ^o
Distilled Water - Kerosene	87
Brine - Kerosene	82
Distilled Water- Mineral Oil	81
Brine - Mineral Oil	78

4.1.6 The Results For Carbonate Rock – Sample 536

The results of Thin Layer Wicking Experiments in the case of dodecane and test liquids - distilled water, brine, kerosene - for carbonate rock, (sample 536), are given in Figure 4.11. and the results for mineral oil and crude oil are given in Figure 4.12. It can be seen that the four liquids have similar wetting tendencies. In addition, crude oil has a very long wicking time.

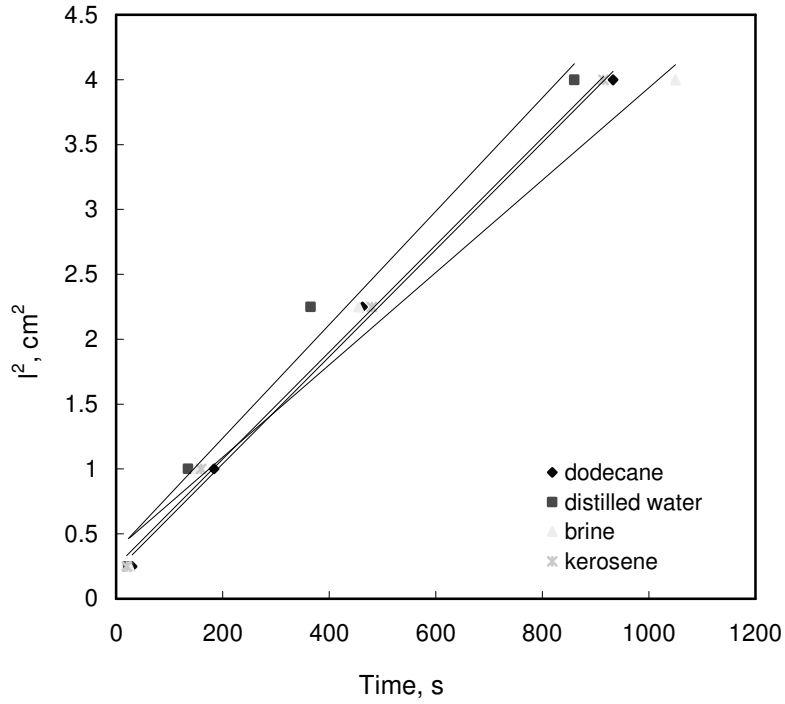

Figure 4.11 : The Results of Wicking Experiments for Dodecane, Distilled Water, Brine and Kerosene on Carbonate Rock 536

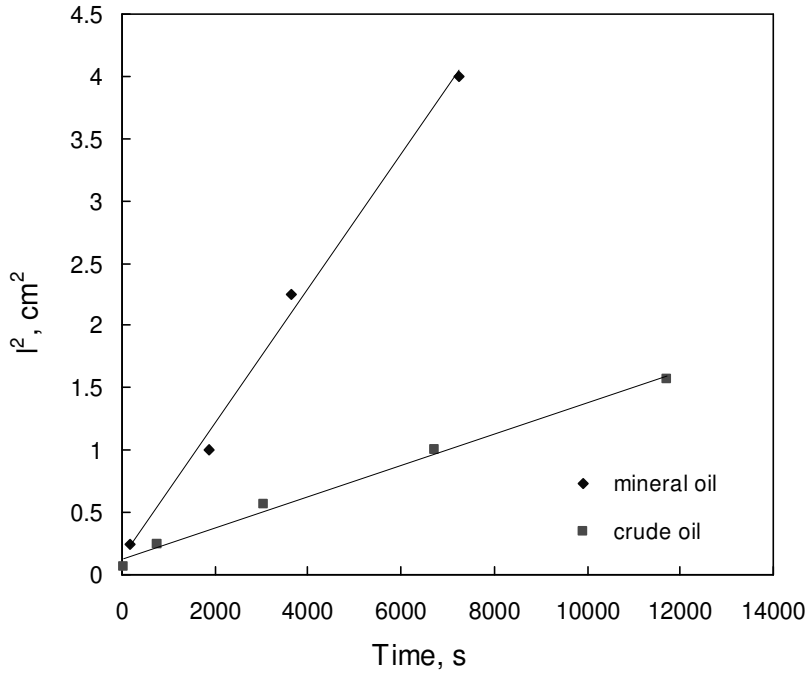

Figure 4.12 : The Results of Wicking Experiments for Mineral Oil and Crude Oil on Carbonate Rock 536

The calculated contact angle values according to test liquid/air/carbonate system are given in Table 4.11. Mineral oil has zero contact angle value which represents complete wetting. While kerosene has lower contact angle values than aqueous phases. In addition, crude oil has the highest contact angle value. Furthermore, the calculated contact angle values according to aqueous phase/oil phase/carbonate system are given in Table 4.12. From these results, it can be concluded that carbonate rock used in this study is oil wet according to the cut-off values cited in the literature (Morrow, 1991).

Table 4.11 : The Calculated Contact Angle Values of Test Liquids for Carbonate Rock 536

Liquids	θ^o
Distilled Water	76
Brine	78
Kerosene	32
Mineral Oil	0
Crude Oil	81

Table 4.12 : The Calculated Contact Angle Values of Liquid-Liquid-Solid Interface for Carbonate Rock 536

Liquids	θ^o
Distilled Water - Kerosene	96
Brine - Kerosene	99
Distilled Water- Mineral Oil	121
Brine - Mineral Oil	134

4.1.7 The Results For Carbonate Rock - Sample703

The results of Thin Layer Wicking Experiments with respect to dodecane and test liquids - distilled water, brine, and kerosene - for carbonate rock (sample 703) are given in Figure 4.13 Furthermore; the results for mineral oil and crude oil are given in Figure 4.14. It can be seen that the four liquids display similar wetting tendencies. In addition, crude oil has high wicking inclination.

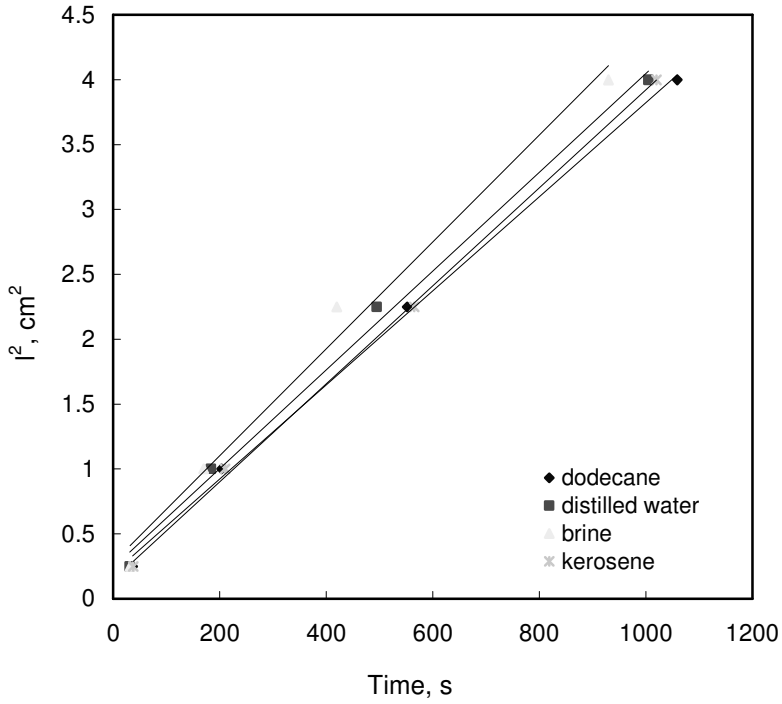

Figure 4.13 : The Results of Wicking Experiments for Dodecane, Distilled Water, Brine and Kerosene on Carbonate Rock 703

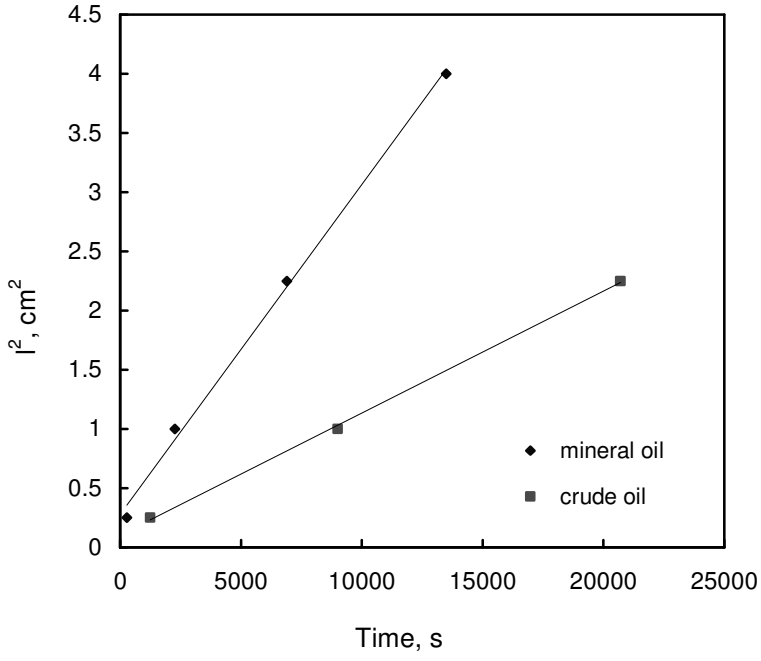

Figure 4.14 : The Results of Wicking Experiments for Mineral Oil and Crude Oil on Carbonate Rock 703

The calculated contact angle values according to test liquid/air/carbonate system are given in Table 4.13. Kerosene and mineral oil have lower contact angle values than aqueous phases. In addition, crude oil has highest contact angle value. Furthermore, the calculated contact angle values according to aqueous phase/oil phase/carbonate system are given in Table 4.14. From these results, it can be concluded that carbonate rock used in this study is oil wet according to the cut-off values cited in the literature (Morrow, 1991).

Table 4.13 : The Calculated Contact Angle Values of Test Liquids for Carbonate Rock 703

Liquids	θ^o
Distilled Water	76
Brine	74
Kerosene	24
Mineral Oil	36
Crude Oil	81

Table 4.14 : The Calculated Contact Angle Values of Liquid-Liquid-Solid Interface for Carbonate Rock 703

Liquids	θ^o
Distilled Water - Kerosene	98
Brine - Kerosene	95
Distilled Water- Mineral Oil	103
Brine - Mineral Oil	106

4.2 The Comparison of the Standard Liquids

Experiments were conducted with heptane, octane, decane, and dodecane due to their low surface tension and apolarity. Taking into account volatility and viscosity, dodecane that gives the highest value of $r^*\cos\theta$ was selected as the standard liquid, and all calculations were performed with its r^* value. It has been observed that there was a rapid evaporation of octane and heptane from the surface during the penetration process. This can negatively affect the penetration rate and cause erroneous values of r^*. Therefore the effect of evaporation should be handled seriously if octane and heptane

wanted to be used in wicking experiments. It was also observed that calculations of contact angles with respect to dodecane gave better results than calculations of contact angles with respect to apolar liquids. This deduction can be seen in Table 3.13.

4.3 The Results of Surface Free Energy Components

The calculated surface free energy components of calcite and glass were given in Table 4.15. According to Karaguzel (2005), when hydrophobicity increases the Lifshitz van der Waals interaction energy increases, because it replaces the place of acid-base energy components. From Table 4.15, it can be seen that calcite has a higher γ_S^{LW} value and lower γ_S^{AB} value than glass. This proves that calcite is more hydrophobic than glass. Moreover, the results show that calcite has higher solid-liquid interfacial tension than glass which means that calcite needs more energy to form unit solid-liquid interface. This also leads to a more hydrophobic surface. The conclusion that calcite is more hydrophobic than glass is in well agreement with the result obtained with contact angle calculations using thin layer wicking method.

Table 4.15 : The Surface Free Energy Components of Calcite and Glass

Samples	γ_S	γ_S^{LW}	γ_S^{AB}	γ_S^{+}	γ_S^{-}	γ_{SL}
Calcite	36.61	29.17	7.44	0.68	20.36	4.57
Glass	49.54	21.48	28.06	7.08	27.80	-1.56

5. CONCLUSIONS

The application of the Washburn equation is a very useful approach to quantify the wettability of a porous core sample with heterogeneous mineralogical composition available in powdered form.

Powdered sample of quartz mineral was proved to be more water-wet than powdered sample of calcite mineral. Furthermore; the contact angle values of carbonates are closer to that of calcite while the contact angle values of Berea and Bentheim sandstone and ground glass are closer to that of quartz.

This study is the first Thin Layer Wicking study in Petroleum and Natural Gas Engineering field and it can be a leading survey to attempt new investigations in this subject.

The contact angle values obtained from Thin Layer Wicking Experiments and the goniometric results are found to be in good agreement with the literature.

Specific to the mineral and rock samples used in this study, quartz mineral is found to be strongly water wet whereas the sandstone samples and glass are found to be water wet according to the cut off values cited in the literature.

Specific to the mineral and rock samples used in this study, the calcite mineral is found to be intermediate water wet and the carbonates are found to be oil wet according to the cut off values cited in the literature.

The surface free energy values of calcite and glass are in good agreement with the values found in the literature. According to the calculated surface free energy components calcite is proved to be more hydrophobic than glass. This conclusion fits with the results obtained from contact angle calculations by using Thin Layer Wicking technique.

Dodecane is found to be the most suitable alkane to be used as a standard liquid for effective pore radius measurements in Thin Layer Wicking experiments.

6. RECOMMENDATIONS

Thin Layer Wicking Method has been proved to provide clearly acceptable and consistent results of advancing contact angles measured on the powdered samples.

The importance of interfacial tension and viscosities of standard and test liquids on Thin Layer Wicking experiments should be well understood and the effects of temperature and humidity should not be ignored.

Extreme care should be applied when handling the samples to not let any purities mix into the powder samples. Also, all equipments especially glass slide should be cleaned thorougly.

The direct inhalation of alkanes should be avoided due to their hazardous vapor therefore throughout the each experiment the laboratory should be well ventilated.

The relationship of wettability with surface free energy can be further investigated.

For future studies, the relation between the contact angles measured using Thin Layer Wicking Method, and the values of wettability measured by other methods used in petroleum industry (e.g. Capillary rise) is of special interest.

Spontaneous imbibition can be studied with the same rock samples and a correlation can be formed between powder wicking and spontaneous imbibition.

Alteration of wettability by changing brine composition and rock type and using different type of crude oil from different formations, furthermore the effect of the temperature on the contact angle can also be studied by Thin Layer Wicking Technique.

REFERENCES

Adam, N.K., 1956., *Physical Chemistry*, Oxford University Press, London.

Adamson, A.W., 1990. *Physical Chemistry of Surfaces*, John Wiley & Sons, Inc., Los Angeles, California.

Amott, E., 1959. Observations Relating to the Wettability of Porous Rock, *Petroleum Transactions, AIME*, **216**, 156-162.

Anderson, W.G., 1986. Wettability literature survey-Part 1: Rock/oil/brine interactions and the effects of core handling on wettability, *Journal of Petroleum Technology*, 1125-1144.

Anderson, W.G., 1986. Wettability literature survey-Part 2: Wettability measurement, *Journal of Petroleum Technology*, 1246-1262.

Asmatalu,R., 2002. Enhancement of the Dewetability Characteristics of Fine Silica Particles, *Turkish J. Eng. Env. Sci*., **26**, 513-519.

Bartell, F.E. and Miller, F.L., 1928, Degree of Wetting of Silica by Crude Petroleum Oils, *Ind. Eng. Chem*., July, **20(7)**, 738-742.

Benner, F.C. and Bartell, F.E., 1942, The Effect of Polar Impurities Upon Capillary and Surface Phenomena in Petroleum Production, *Drill. And Prod. Prac.*, API, New York City, 341-348.

Browns, R.J.S. and Fatt, I., 1956, Measurements of Fractional Wettability of Oilfield Rocks by the Nuclear Magnetic Relaxation Method, *Trans. AIME*, **207**, 262-264.

Chen, D. and McMorran, D., 1999. Use of the DCA technique to measure the wettability of porous materials, *American Laboratory*, 35-37.

Cuiec, L.E., 1990. Evaluation of Reservoir Wettability and Its Effect on Oil Recovery, Interfacial Phenomena in Oil Recovery, N.R. Morrow (ed.), Marcell Dekker, New York, 319-75.

Donaldson, E.C., Thomas, R.D., and Lorenz, P.B., 1969. Wettability Determination and Its Effect on Recovery Efficiency, *SPEJ*, 13-20.

Eustathopoulos, N., Nicholas, M.G. and Drevet, B., 1999. *Wettability at High Temperatures*, Pergamon Materials Series, Oxford, 43-52.

Fatt, I. and Klikoff, W.A., 1959, Effect of Fractional Wettability on Multiphase Flow Through Porous Media, *Trans. AIME*, **216**, 426-432.

Francisca, F. M., Rinaldi, V. A., and Santamarina, J. C., 2003. Instability of hydrocarbon films over mineral surfaces: Microscale experimental studies, *Journal of Environmental Engineering*, 1120-1128.

Giese, R.F., van Oss, C.J., 2002. *Colloid and Surface Properties of Clays and Related Minerals*, Surfactant Science Series, **105**, Marcel Dekker inc. New York.

Good, R.J., van Oss, C.J., 1992. in *Modern Approaches to Wettability: Theory and Applications,* M.Shrader and G. Loeb (Eds), 1-27, Plenum Press, New York.

Gökmen, M., 2003. Şekil Faktörü, Karakteristik Uzunluk ve Sınır Koşullarının Doğal Su İmbibisyonuna Etkileri, *Ms. Thesis,* İ.T.Ü. Institude of Science and Technology, İstanbul.

Holysz, L., 1998. Surface Free Energy Components of Silica Gel Determined by the Thin Layer Wicking Method for Different layer Thickness of Gel, *Journal of Materials Science*, **33**, 445-452.

Iwankow, E.N., 1960, A Correlation of Interstitial Water Saturation and Heterogeneous Wettability, *Producers Monthly*, **24**, October, 18-26.

Jackson P.V., Hunt, J.A., Doherty, P.J., 2004. Hydrophilicity of 3-D Biomaterials: The Washburn Equation, *J. of Materials Science*, **15**, 507-511.

Jadhunandan, P.P., 1990. Effects of Brine Composition, Crude Oili and Aging Conditions onWettability and Oil Recovery, *Ph.D. Thesis*, New Mexico Inst. Of Minig and Tech.

Karagüzel, C., 2005. Na-K Feldspat Minerallerinin Flotasyon Yöntemi ile Ayrımında Hidrofobisiteyi Etkileyen Parametreler, *Ph.D. Thesis*, İ.T.Ü., İstanbul.

Karagüzel, C., Can, M.F., Sönmez, E., Çelik, M.S., 2005. Effects of electrolyte on Surface Free Energy Components of Feldspar Minerals Using Thin-Layer-Wicking Method, *J. of Colloid and Interface Science*, **285**, 190-200.

Kumbasar, I., Aykol, A., 1993. Mineroloji, İ.T.Ü, Teknik Üniversite Matbaası, Gümüşsuyu, İstanbul.

Kwok, D.Y., Wu, R., Li, A., Neumann, A.W., 2000. Contact Angle Measurements and Interpretation: Wetting Behavior and Surface Tensions for Poly(alkyl methacrylate) Polymers, *J. Adhesion Sci. Technol.*, **14(5)**, 719-743.

Ma, S., Morrow, N.R., 1991. Effect of Firing on Petrophysical Properties of Berea Sandstone, *SPEJ*, 21045, 447- 456.

Ma, S., Morrow, N.R., Zhou, X., and Zhang, X., 1994. Characterization of Wettability from Spontaneous Imbibition Measurements, *paper CIM 94-47, Petr. Soc. of CIM Ann. Tech. Meeting*, Calgary, June, 12-15.

Marmur A., 1992. *Penetration and Displacement* in Capillary Systems in Modern Approach to Wettability: Theory and Application, edited by M.Shrader and G. Loeb (Eds), 327-358, Plenum Press, New York.

Marsden, S.S. and Nikias, P.A., 1962, The Wettability of the Bradford Sand. I., *Producers Monthly*, May, 2-5.

Michel, J. C , Riviere, L. M., and Bellon-Fontaine, M. N., 2001. Measurement of the wettability of organic materials in relation to water content by the capillary rise method, *Europian Journal of Soil Science*, **52**, 459-467.

Morrow, N. R., 1975. The effects of surface roughness on contact angle with special reference to petroleum recovery, *The Journal of Canadian Petroleum Technology*, 1-12.

Morrow, N. R., 1990. Wettability and Its Effect on Oil Recovery, *The Journal of Petroleum Technology*, 1476-1484.

Morrow, N.R., Lim, H.T. and Ward, J.S., 1986, Effect of Crude-Oil-Induced Wettability Changes on Oil Recovery, *SPE Formation Evaluation*, February, 89-103.

Morrow, N.R., Mason, G. 2001. Recovery of Oil by Spontaneous Imbibition, *Current Opinion in Colloid & Interface Science*, **6**, 321-337.

Owens, D.K., Wendt R.C., 1969. *J. Applied Polym. Sci.* **13**, 1741.

Salathiel, R.A., 1973, Oil Recovery by Surface Film Drainage in Mixed Wettability Rocks, *J. Pet. Tech*., October, 1216-1224.

Schultz, J., Nardin, M., 1992. *Determination of the Surface Energy of Solids by the Two-Liquid-Phase Method* in Modern Approach to Wettability: Theory and Application, edited by M.Shrader and G. Loeb (Eds), 327-358, Plenum Press, New York.

Swanson, R. E., 1976. The influence of molecular structure of vapor phase chemisorbed Fatty acids. Present in fractional monolayer concentrations on the wettability of cellulose film, *The Institute of Paper Chemistry*, 6-26.

Tajibaev, R., 2004. The Contact Angle as a Wettability Measurement- Thin Layer Wicking Approach, *Graduation Design Project*, İ.T.Ü., İstanbul.

Ucko, D.A., 1982, Basics for Chemistry, Academic Press., Orlando, Florida, 416-427.

Van Oss, C.J. 1994. *Interfacial Forces in Aqueous Media*. Marcel Dekker, Inc., New York, USA, 21-98.

Van Oss, C.J., Chaudhury, M.k., Good, R.J., 1988. *J. Of Colloid and Interface Science*, **128**, 313.

Washburn, E. W., 1921. The physical review. The dynamics of capillary flow, *Second Series*, **17(3)**, 273-283.

Wolfrom, R. L., Chander, S. and Hogg, R., 2002. Evaluation of capillary rise methods for determining wettability of powders, *Minerals and Metallurgical Processing*,**19**, 198-202.

Wu, W., 2001. Baseline studies of the clay minerals society source clays: Colloid and surface phenomena, *Clays and Clay Minerals*, **49**, 446-452.

Yıldırım, I. 2001. Surface Free Energy Characterization of Powders, The Virginia Polytechnic Institute, *Ph.D Dissertation*, Mining and Minerals Engineering, Blacksburg, Virginia, USA, 51-77.

Yıldız, H.Ö., 1998, PT 703 Enhanced Oil Recovery Study Notes, ITU Petroleum and Natural Gas Engineering Deparment, İstanbul.

Yıldız, H.Ö., Gökmen, M., 2001. An Investigation of Capillary and Viscous Forces for Very Strongly Water Wet Systems, *Petroleum Society*, **133**, Canada.

Zhou, X., Morrow, N.R., and Ma, S., 1996. Interrelationship of Wettability, Initial Water Saturation, Aging Time, and Oil Recovery by Spontaneous Imbibition and Waterflooding, *paper SPE 35436 presented at the SPE/DOE Tenth Symposium on Improved Oil Recovery*, Tulsa, Oklahoma, April, 21-24.

Zisman W.A., 1944. Relation of the Equilibrium contact Angle to Liquid and Solid Constitution, *Advances in Chemistry Series*, **43**, 1-48.

APPENDIX-A. WICKING TIME VERSUS L^2 FOR SAMPLES

Table A.1 : Wicking Time versus l^2 For Quartz Sample

		Wicking Time for Test Liquids, (t, seconds)				
Distance, l, cm	**l^2, cm^2**	Dodecane	D. water	Brine	Kerosene	Mineral oil
0,5	0,25	10	6	6	10	48
1	1	40	16	16,5	46	310
1,5	2,25	106	34	35	101	960
2	4	184	59	63	190	1740

Table A.2 : Wicking Time versus l^2 For Glass Sample

		Wicking Time for Test Liquids, (t, seconds)				
Distance, l, cm	**l^2, cm^2**	Dodecane	D. water	Brine	Kerosene	Mineral oil
0,5	0,25	4	2	3	3	17
1	1	12	6	6	9	128
1,5	2,25	27	11	11	18	285
2	4	52	19	21	35	575

Table A.3 : Wicking Time versus l^2 For Berea Sandstone Sample

		Wicking Time for Test Liquids, (t, seconds)				
Distance, l, cm	**l^2, cm^2**	Dodecane	D. water	Brine	Kerosene	Mineral oil
0,5	0,25	8	7	4	7	65
1	1	36	17	15	28	385
1,5	2,25	78	34	30	68	960
2	4	140	54	54	120	1680

Table A.4 : Wicking Time versus l^2 For Bentheim Sandstone Sample

		Wicking Time for Test Liquids, (t, seconds)				
Distance, l, cm	**l^2, cm^2**	Dodecane	D. water	Brine	Kerosene	Mineral oil
0,5	0,25	31	16	17	26	390
1	1	161	79	84	153	1920
1,5	2,25	382	175	205	358	4980
2	4	738	355	405	660	9600

Table A.5 : Wicking Time versus l^2 For Calcite Sample

		Wicking Time for Test Liquids, (t, seconds)				
Distance, l, cm	**l^2, cm^2**	Dodecane	D. water	Brine	Kerosene	Mineral oil
0,5	0,25	20	16	13	20	183
1	1	85	48	52	78	985
1,5	2,25	191	110	103	168	2740
2	4	336	205	198	295	5700

Table A.6 : Wicking Time versus l^2 For Carbonate Rock Sample 536

		Wicking Time for Test Liquids, (t, seconds)				
Distance, l, cm	**l^2, cm^2**	Dodecane	D. water	Brine	Kerosene	Mineral oil
0,5	0,25	30	23	25	20	165
1	1	184	135	151	160	1860
1,5	2,25	463	365	455	480	3624
2	4	933	860	1050	915	7250

Table A.7 : Wicking Time versus l^2 For Carbonate Rock Sample 703

		Wicking Time for Test Liquids, (t, seconds)				
Distance, l, cm	**l^2, cm^2**	Dodecane	D. water	Brine	Kerosene	Mineral oil
0,5	0,25	37	31	32	38	285
1	1	203	184	170	210	2260
1,5	2,25	552	495	420	565	6900
2	4	1059	1005	930	1020	13500

Table A.8 : Wicking Time versus l^2 For Crude Oil

		Wicking Results for Crude Oil			
Distance, l, cm	**l^2, cm^2**	**Berea**	**Calcite**	**Carbonate-536**	**Carbonate-703**
0,25	0,06	–	–	36	–
0,5	0,25	82	400	775	1240
0,75	0,56	–	–	3060	–
1	1,00	465	1800	6720	9000
1,25	1,56	–	–	11700	–
1,5	2,25	1119	3615	–	20700
2	4,00	2220	7272	–	–

CURRICULUM VITAE

Fatma Bahar Öztorun was born in 1981, İstanbul. She graduated from Petroleum and Natural Gas Engineering programme at Istanbul Technical University in 2003. She is still taking her master programme in Petroleum and Natural Gas Engineering at ITU. She has been a research assistant in the same department since February 2005.